BLANKET ENGINEERING

KEYWORDS: *safety factors, fusion integral experiments, neutronics R&D*

FUSION INTEGRAL EXPERIMENTS AND ANALYSIS AND THE DETERMINATION OF DESIGN SAFETY FACTORS—I: METHODOLOGY

M. Z. YOUSSEF, A. KUMAR, and M. A. ABDOU
University of California, Los Angeles, School of Engineering and Applied Science
Mechanical, Aerospace, and Nuclear Engineering Department
Los Angeles, California 90095

Y. OYAMA and H. MAEKAWA *Japan Atomic Energy Research Institute*
Department of Reactor Engineering, Tokai Research Establishment
Tokai-mura, Naka-gun, Ibaraki-ken 319-11 Japan

Received January 28, 1994
Accepted for Publication July 28, 1994

The role of the neutronics experimentation and analysis in fusion neutronics research and development programs is discussed. A new methodology was developed to arrive at estimates to design safety factors based on the experimental and analytical results from design-oriented integral experiments. In this methodology, and for a particular nuclear response, R, a normalized density function (NDF) is constructed from the prediction uncertainties, u_i's, and their associated standard deviations, $\pm\sigma_i$'s, as found in the various integral experiments where that response, R, is measured. Important statistical parameters are derived from the NDF, such as the global mean prediction uncertainty, $\bar{u}$, and the possible spread, $\pm\sigma_u$, around it. The method of deriving safety factors from many possible NDFs based on various calculational and measuring methods (among other variants) is also described. Associated with each safety factor is a confidence level, designers may choose to have, that the calculated response, R, will not exceed (or will not fall below) the actual measured value. An illustrative example is given on how to construct the NDFs. The methodology is applied in two areas, namely the line-integrated tritium production rate and bulk shielding integral experiments. Conditions under which these factors could be derived and the validity of the method are discussed. The described methodology could be applied to the integral experiments proposed for the International Thermonuclear Experimental Reactor (ITER) neutronics research and development, particularly, in deriving the required safety factors for ITER shielding.

I. INTRODUCTION

Quite often, nuclear designers rely on performing designated integral experiments prior to the construction of a nuclear reactor to validate the analytical and computational tools and nuclear data used in predicting key neutronics parameters in a component that is part of the final design. This practice in some cases is deemed necessary since the comparison between measured data and analytical prediction could in principle reveal discrepancies whose sources can be eliminated by either improving a particular nuclear data set or further developing the transport codes applied to meet higher prediction accuracy. Clearly the decision of launching an experimental program depends largely on the cost/benefit involved on the safety, direct, and indirect cost of the reactor. Alternatively, in the case of not conducting integral experiments for the purpose of improving database/design codes, it is a common practice to apply correction (safety) factors, derived from these integral experiments, to the calculated nuclear response under investigation. These design margins cover the several sources of uncertainties arising from the approximations in the calculational model used, nuclear data uncertainties, and approximations embedded in the transport method applied.

In this paper, we outline a new methodology that can be applied to the prediction uncertainty of a nuclear response, R, and the associated standard deviation as they are estimated in an integral experiment, among many other similar experiments, to arrive at estimates to design safety factors that designers can use to ensure that the calculated response, R, is in agreement with the actual measured value. Conditions that influence the estimation of these factors are pointed out. The inter-relation between the planning/needs and the outcomes of integral experiments and the design/construction of fusion reactors are first discussed in Sec. II. The proposed methodology and an example on how to apply it are discussed in Secs. III and IV, respectively. In Sec. V, we give two specific applications on deriving safety factors from tritium production rate and bulk shielding experiments. The validity of the proposed methodology is discussed in Sec. VI, while the concluding remarks from this work are given in Sec. VII.

II. THE ROLE OF NEUTRONICS EXPERIMENTATION IN A FUSION NEUTRONICS RESEARCH AND DEVELOPMENT PROGRAM

There are a number of neutronics issues that need to be addressed via an aggressive research and development (R&D) program. Important design responses of interest are shielding of sensitive nuclear components, personnel and radiological doses around the reactor, tritium production rate in the blanket that satisfies tritium self-sufficiency,[1] nuclear heat generation and associated profiles, induced radioactivity, and decay heat. The main elements of the R&D program that ensures that the prediction accuracies of these nuclear responses are within tolerable levels through well-assessed design margins are the following:

1. basic nuclear data measurements and evaluation
2. nuclear data processing and generation of transport/response working data libraries
3. transport and response codes development
4. integral experiments and analyses
5. experimental and measuring techniques development.

Generally, the main objectives of the R&D program are the following:

1. to provide the experimental database required for approval and licensing of the device
2. to verify the prediction capabilities and generation of design safety factors
3. to reduce the high cost associated with large safety factors used to compensate for uncertainties.

Figure 1 shows the inter-play between the elements of the R&D program and the nuclear design of a reactor.

There has been an extensive effort in the area of differential data measurements[2,3] with the objective of either improving previously existed data or generating new data to meet particular accuracies, as recommended by the fusion data community.[4,5] These basic measured and/or evaluated data constitute now a number of the latest databases among which are ENDF/B-VI, JENDL-3, JEF-2, BROND, and CENDL. These databases are processed into pointwise and multigroup transport/response data libraries for use by blanket/shield designers. The FENDL library is based on all these databases and is in the process of preparation by the International Atomic Energy Agency (IAEA) (Ref. 6). The working libraries (e.g., EFF-1, EFF-2, MATXS, etc., see Fig. 1) are used directly by analysts along with the appropriate transport/response code. As for the transport codes based on deterministic methods, there are several of them available such as DOT (Ref. 7), TORT and DORT (Ref. 8), 1-, 2-, and 3-DANT (Ref. 9), DOT-DD (Ref. 10), and BISTRO (Ref. 11). Examples of Monte Carlo transport codes are MCNP (Ref. 12), MORSE-DD (Ref. 13), GMVP (Ref. 14), and TRIPOLI (Ref. 15). Examples of codes that are specialized in particular response calculation (e.g., heating rate, activation) are RACC (Ref. 16), DKR-ICF (Ref. 17), KAOS (Ref. 18), and THIDA (Ref. 19). Cross-section sensitivity/uncertainty analysis codes are useful in analyzing integral experiments/design, some examples of which are FORSS (Ref. 20) and SENSIT-2D (Ref. 21).

The integral experiments themselves can be classified as benchmark experiments and engineering-oriented experiments. The first class of experiments are usually simple in geometry and are constituted of single, or at most few material compositions, so as to be best used in validating codes and databases.[22,23] Examples of these experiments are the angular neutron flux measurements on beryllium[24] and lead,[25] the measurements of leakage spectrum from several materials,[26,27] and tritium production rates in lithium spheres.[28] In particular, there have been recent benchmark experiments to examine beryllium data due to its importance in the fusion blanket as a neutron multiplier. Examples of measurements and analysis on beryllium multiplication properties are the manganese bath experiment at INEL (Ref. 29), the Chinese experiments on beryllium shells,[30] and the Karlsruhe experiments on beryllium spheres.[31] Generally, the measured response in these benchmark experiments are in-system and leakage neutron/gamma spectrum, dosimetric reaction rates, and tritium production rates. However, there have been recent measurements on neutron and gamma heating[32-34] to validate the karma factors[35,18] used in the calculations of the heat deposition rate by designers. Furthermore, measurements and analysis on induced radioactivity and gamma decay have been conducted recently.[36,37] Cross-section sensitivity and

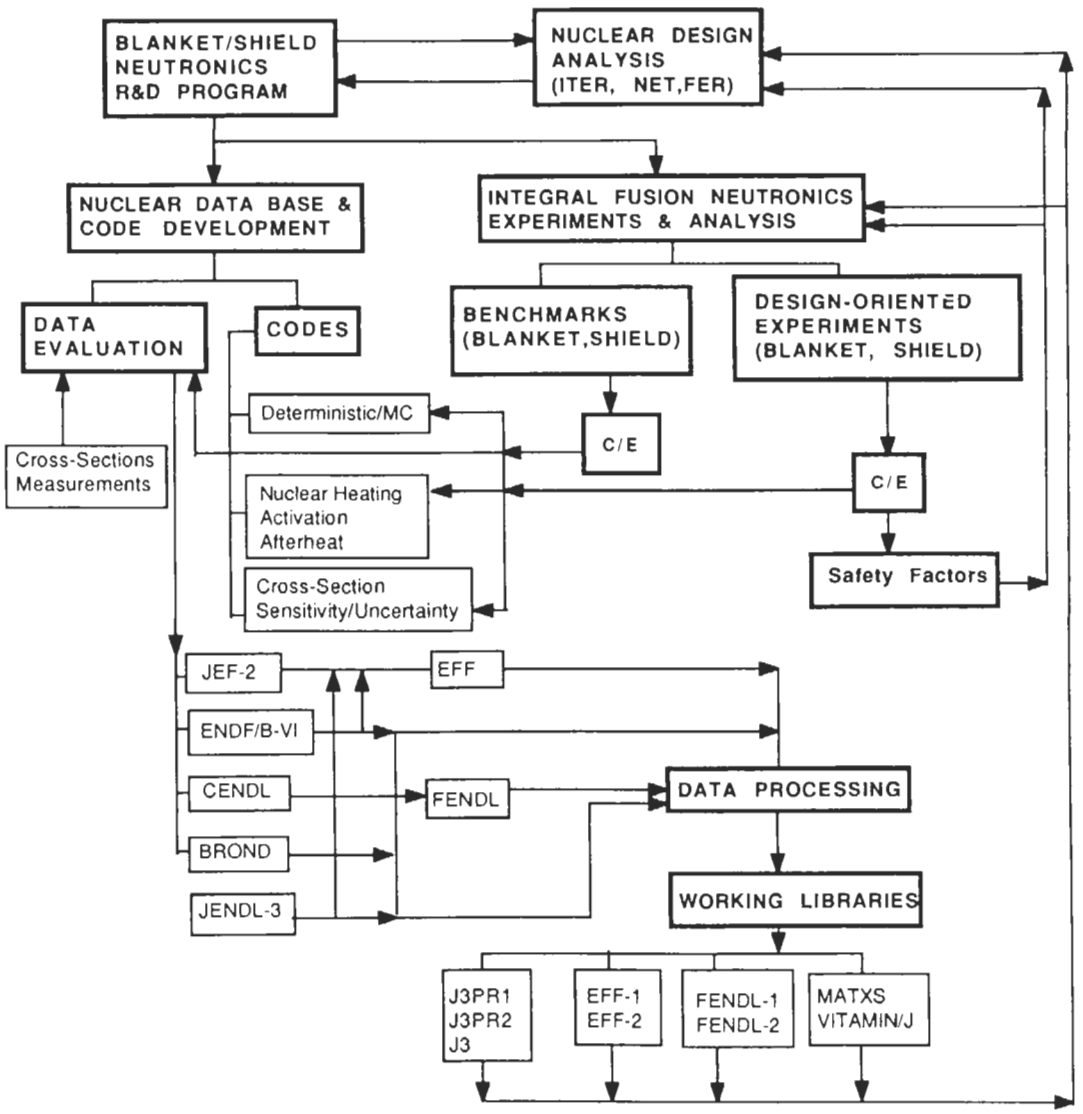

Fig. 1. Inter-relationship between fusion nuclear design analysis and blanket/shield neutronics R&D.

uncertainty analysis to this class of experiments is, in many cases, the key to identifying the deficiencies in nuclear data.[38,39]

The engineering-oriented integral experiments, on the other hand, simulate, in some detail, the engineering features of a fusion blanket/shield module found in a fusion reactor. This includes, the first wall, coolant channels, a neutron multiplier, etc., in a blanket, and/or gap/slits, and multi-layer of materials with different shielding capabilities in a shield module. Some other features may intentionally be preserved such as simulating a partial or full coverage of the test assembly relative to the 14-MeV incident neutron source and simulating the energy and angular distributions of the incident source found in a fusion reactor. The main objectives of this class of experiments are to evaluate the over-all potential of a particular blanket type (e.g., breeding material) in functioning as prediction indicates, on one hand, and to evaluate the mean prediction uncertainties in key nuclear responses and to generate design safety factors for designers, on the other. This later objective is the subject of this paper. Examples of dedicated programs that focus on this class of experiments are the U.S. DOE/JAERI collaborative program on fusion neutronics,[40-49] and the experiments at the LOTUS facility, Switzerland.[50,51] Table I gives the specifications of the leading 14-MeV neutron source facilities available worldwide and those used in these experiments.

III. A METHODOLOGY FOR EVALUATING DESIGN SAFETY FACTORS FROM ENGINEERING-ORIENTED FUSION INTEGRAL EXPERIMENTS

Suppose we have the calculational and experimental results from an N number of experiments. In a given experiment, i, a particular integral nuclear response, R,

TABLE I

Leading Neutron Source Facilities

Facility	Location	Mode of Operation	Type	Source Intensity
FNS	JAERI (Japan)	Pulsed	Point	3×10^{11} and 5×10^{12} n/s
		Continuous	Simulated line source	3×10^{11} n/s
FNG (Ref. 52)	Frascati (Italy/EC)	Pulsed Continuous	Point	5×10^{11} n/s
TUD	Dresden (Germany/EC)	Pulsed Continuous	Point	2×10^{11} n/s
Other Facilities Available				
Switzerland:	LOTUS, S ~ 5×10^{12} n/s (Ref. 50)			
Japan:	OKTAVIAN, Osaka University, S ~ 5×10^{11} n/s (Ref. 53)			
Germany:	KfK, Karlsruhe, S ~ 10^9 n/s (Ref. 31)			
Russia:	IAE, Kurchatov, Moscow, S ~ 5×10^{10}/s (Ref. 54)			
	MEPI, Moscow, S ~ 5×10^{10} n/s (Ref. 54)			
	KPI, Moscow, S ~ 5×10^{10} n/s (Ref. 54)			
China:	SWINPS, Chengdu, S ~ 10^9 n/s (Ref. 30)			
USA:	ORNL, Oak Ridge, S ~ 10^{10} n/s			
	ANL, S ~ 10^{10} n/s			
	INEL, Idaho, S ~ 10^8 n/s (Ref. 29)			

has a calculated value, c_i, and a measured value, e_i. If the calculational method and modeling used to arrive at c_i are exact using the most accurate database and if no experimental errors are encountered, the ratio c_i/e_i should be unity. However, due to the approximations embedded in the calculational method used and the inaccuracies encountered in the database and/or modeling, the ratio c_i/e_i deviates from unity by a fraction, $u_i = c_i/e_i - 1$. This fraction is defined as the prediction uncertainty in the response R. The relative variance, σ_{ir}^2, in u_i (or the ratio c_i/e_i) is evaluated from the calculational and experimental errors (relative variances, σ_{cir}^2 and σ_{cir}^2) as follows:

$$\sigma_{ir}^2 = \sigma_{cir}^2 + \sigma_{eir}^2 \ , \qquad (1)$$

where σ_{cir}^2 and σ_{cir}^2 are given by σ_{ci}^2/c_i^2 and σ_{ei}^2/e_i^2, respectively, and σ_{ci} and σ_{ei} are the standard deviations (errors) in c_i and e_i, respectively. The calculational error could include uncertainties due to geometrical modeling, assumptions embedded in the transport calculations used, and uncertainties associated with nuclear data. The experimental errors could include the systematic errors arising from measurements using particular measuring techniques. The standard deviation in the quantity u_i is thus given by $\sigma_i = \sigma_{ir} \cdot (c_i/e_i)$ and the extremes around the mean value u_i are given by the $u_{imax} = u_i + \sigma_i$ and $u_{imin} = u_i - \sigma_i$.

Suppose we divide the space of the prediction uncertainty, u, into intervals, Δu, and ask what fraction of experiments, among the total number of experiments, N, have prediction uncertainty in any particular interval. An experiment is counted toward that fraction when its u_{imax}, u_{imin}, or both, lie within the interval boundaries u and $u + \Delta u$, or when the boundaries u and $u + \Delta u$ lie within the boundaries u_{imin} and u_{imax}. Thus, we define the normalized density function f(u) such that the quantity $Nf(u)\Delta u$ is the number of experiments whose prediction uncertainty u in the response R is within the interval between u and $u + \Delta u$. The normalized density function f(u) is thus a histogram that could approach a smooth curve as $N \to \infty$ and $\Delta u = du \to 0$. In this case, the mean value, $\bar{u}$, of the prediction uncertainty in the response R among all the experiments considered is evaluated from

$$\bar{u} = \int_{-1}^{\infty} uf(u)\,du \ , \qquad (2)$$

and the normalization condition is given by

$$\int_{-1}^{\infty} f(u)\,du = 1 \ . \qquad (3)$$

The lower boundary of $u = (c/e) - 1$ is -1 (when $c = 0$) and the upper boundary is ∞ (when $c \to \infty$). In practice, the total number of experiments N is limited and a finite interval width, Δu, is used. The mean prediction uncertainty, $\bar{u}$, is thus obtained from the normalized density function (NDF), f_j, as follows

$$\bar{u} = \sum_{j=1}^{j=K} uf_j \ , \qquad (4)$$

and the normalization condition is given by

$$\sum_{j=1}^{j=K} f_j = 1 \ , \tag{5}$$

where K is the total number of intervals, j, of a width, Δu_j considered between predetermined upper and lower bounds, U(max) and U(min), and the quantity Nf_j is the number of experiments whose prediction uncertainty in the response R lies within the uncertainty interval boundaries u_j and $u_j + \Delta u_j$. The average of the square of u is defined as

$$\overline{u^2} = (u_{rms})^2 = \sum_{j=1}^{j=K} u^2 f_j \ . \tag{6}$$

The standard deviation, σ_u, is defined as

$$\sigma_u = \left[\sum_{j=1}^{j=K} (u - \bar{u})^2 f_j \right]^{1/2} \ , \tag{7}$$

and it gives the spread around the mean value $\bar{u}$. It can be shown that

$$\sigma_u = [\overline{u^2} - \bar{u}^2]^{1/2} \ , \tag{8}$$

where $\bar{u}^2$ is the square of the mean prediction uncertainty $\bar{u}$. The most probable value for the prediction uncertainty, u_{mp}, is defined as the value of u at which the normalized density function has its largest value. The value of u_{mp} is not necessarily the same as the average value $\bar{u}$. The case $u_{mp} = \bar{u}$ is true in Gaussian distribution.

Figure 2 shows an example of a possible NDF, f_j, for a nuclear response R (in the figure, u is presented in fraction). Also shown is a Gaussian density function that has the same mean, $\bar{u}$, and the same standard deviation, σ_u. The area under both distributions is unity. The resemblance between the two distributions could improve as the number of experiments considered increases. Note that the NDF, in the limit, is not necessarily a Gaussian distribution (see Sec. VI).

From the figure, it is most likely that the calculated value, c, of the response R will exceed the measured value, e, since the mean value, $\bar{u}$, is positive. However, there is a definite probability that c could also be smaller than e. For a designer, who would like to account for the prediction uncertainties encountered in integral experiments in his design, the seriousness and impact of the fact that the calculated value c could be either larger or smaller than the actual measured value e depends on the nuclear response in hand. For example, if c is larger than e in the case of the tritium production rate, TPR (response R in Fig. 2), this implies that the calculations overpredict the tritium produced in the test assembly. This consequently indicates that the tritium breeding ratio (TBR) in a real fusion blanket may

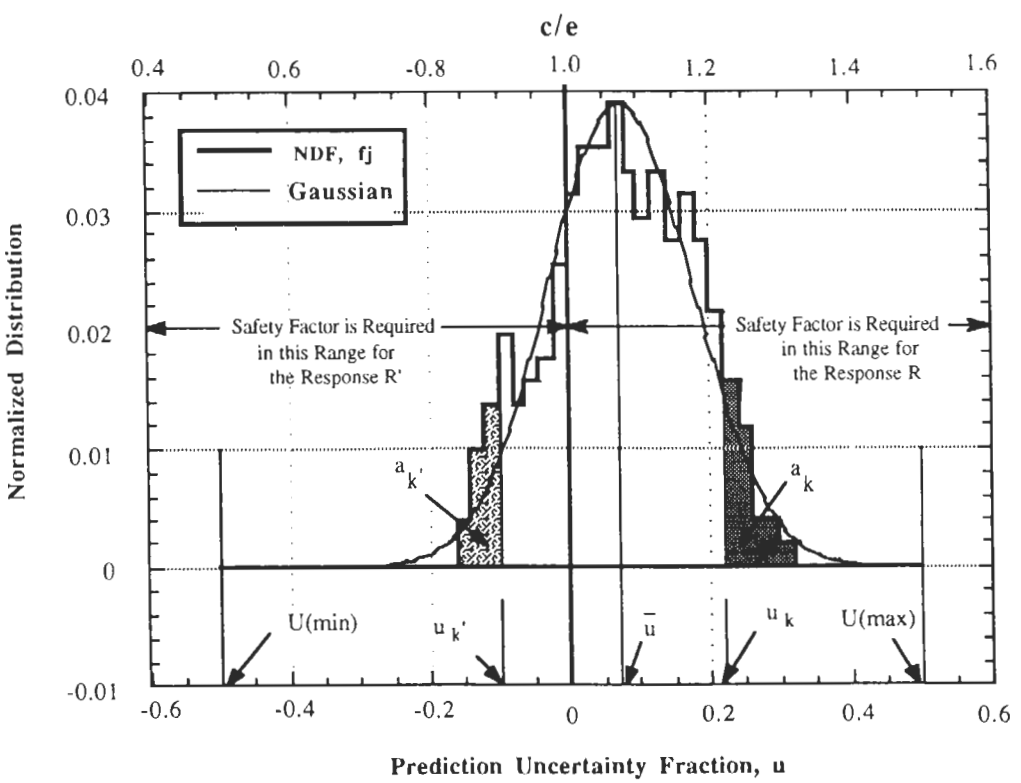

Fig. 2. Example of a normalized density function, f_j, for a nuclear response, R, where a design safety factor is required.

indeed fall below a minimum value dictated by satisfying the tritium self-sufficiency condition.[1] On the other hand, if c is smaller than e in the case of fast neutron fluence behind a bulk shield (response R′ in Fig. 2), this implies that the calculations underpredict the actual nuclear damage that may occur in the superconducting magnet (SCM) located behind the shield.[55–58] In both cases, the designer should apply a safety factor to the calculated response under consideration. To derive this safety factor for the case when overprediction could impose a design concern we notice from Fig. 2 that the probability that the uncertainty in the calculated response R could be larger than a given value, u_k, is expressed by the shaded area, a_k. Thus, by accepting an overprediction in R given by u_k, we are also accepting a risk level (RL), quantified by the quantity a_k, that indeed the overprediction could also be larger than u_k. In other words, our confidence level (CL) that the calculated response R will exceed the measured value by no more than u_k is given by the fraction $(1 - a_k)$. In this case, a designer could reduce his initial calculated value, c_k, by applying a safety factor, S_k, given by

$$S_k = u_k + 1 = c_k/e_k \tag{9}$$

such that the modified calculated response, c_{mk}, is obtained from the relationship

$$c_{mk} = c_k/S_k \ , \tag{10}$$

which implies that the calculated value, c_k, is brought into agreement with the actual measured value, e_k, with an associated confidence level, given by the fraction $(1 - a_k)$, that calculations will not exceed the actual measured value. It is clear, therefore, that the value of the safety factor applied depends on the level of confidence a designer wishes to have in ensuring that the calculated response R will not exceed the actual measured value. Using larger safety factors implies that more conservatism is applied to the design and higher confidence level is achieved in calculating the response in hand.

IV. ILLUSTRATIVE EXAMPLE

The design concern in this example is that calculated values of the response R could be larger than the measured values in the integral experiments considered. Two calculational methods are used to estimate the response, R, namely, calculational methods C1 and C2. The calculations could be performed, for example, by using the DOT transport code[7] based on the discrete ordinates method (C1) and by applying the MCNP (Ref. 12) Monte Carlo code (C2). Other methods could be applied and they are designated as the calculational set $\{C1,C2,\ldots,C_{NC}\}$. Likewise, four measuring methods are used to measure the response, R, and they are designated as the measuring set {M1,M2,M2,M4}, but they could generally be $\{M1,M2,\ldots,M_{NM}\}$. There are 27 experiments for which a comparison was made between the measured and calculated values of the response, R. The experiments are grouped under three distinct geometrical arrangements, {G1,G2,G3}, which could generally describe the overall conditions under which the experiments were conducted (e.g., external 14-MeV point source, external line source, etc.) but generally, several arrangements $\{G1,G2,\ldots,G_{NG}\}$ may be available when the integral experiments are performed.

Figure 3 shows the prediction uncertainty of the response R, u_i, and the spread around it, $\pm\sigma_i$, as obtained in each experiment based on results from the measuring method M1 and the two calculational methods C1 and C2. The identification (G2,EX16,M1), for example, refers to experiment number 16 which is performed under the geometrical condition G2 using measuring technique M1. For this particular experiment, the prediction uncertainty in the response R is estimated based on the calculational methods C1 and C2. Figure 4 gives these prediction uncertainties but based on the measuring methods M2, M3, and M4, separately. Note that the number of cases shown in Fig. 4 for each measuring method is fewer than those shown in Fig. 3, indicating that the response R was not necessarily measured by the four measuring methods in each experiment. Also, each experiment was not necessarily analyzed by the two calculational methods C1 and C2.

Figure 5 shows the histogram of the NDF of the prediction uncertainty, u, based on measuring method M1 and both the calculational method C1 and C2. The mean prediction uncertainty, $\bar{u}$, is ~3% and the standard deviation, σ_u, is ~8.8%. The number of cases considered with this measuring method is 50 (see Fig. 3). The Gaussian curve that has the same mean prediction uncertainty, $\bar{u}$, and standard deviation, σ_u [see Eqs. (4) and (7)], as those of the NDF is also shown in Fig. 5 for comparison.

The relationship between the accepted (adopted) safety factor, S_k, and the associated confidence level, $(CL)_k$, in percentage, is shown in Fig. 6. This relationship is obtained from the NDF shown in Fig. 5 according to the methodology described in the previous section. Also shown is the associated risk level $(RL)_k$ for comparison and it is clear that at any given safety factor S_k, $(CL)_k + (RL)_k = 100\%$. If no safety factor is used ($S_k = 1 = c/e$), the confidence level that calculated response R will not exceed the actual measured value is ~42%.

IV.A. Effect of the Size of the Prediction Uncertainty Interval on the Determination of Safety Factors

The NDF approaches a smooth curve as the number of cases considered $N \to \infty$ and as the uncertainty interval width used to construct the NDF, $\Delta u_j \to 0$. To

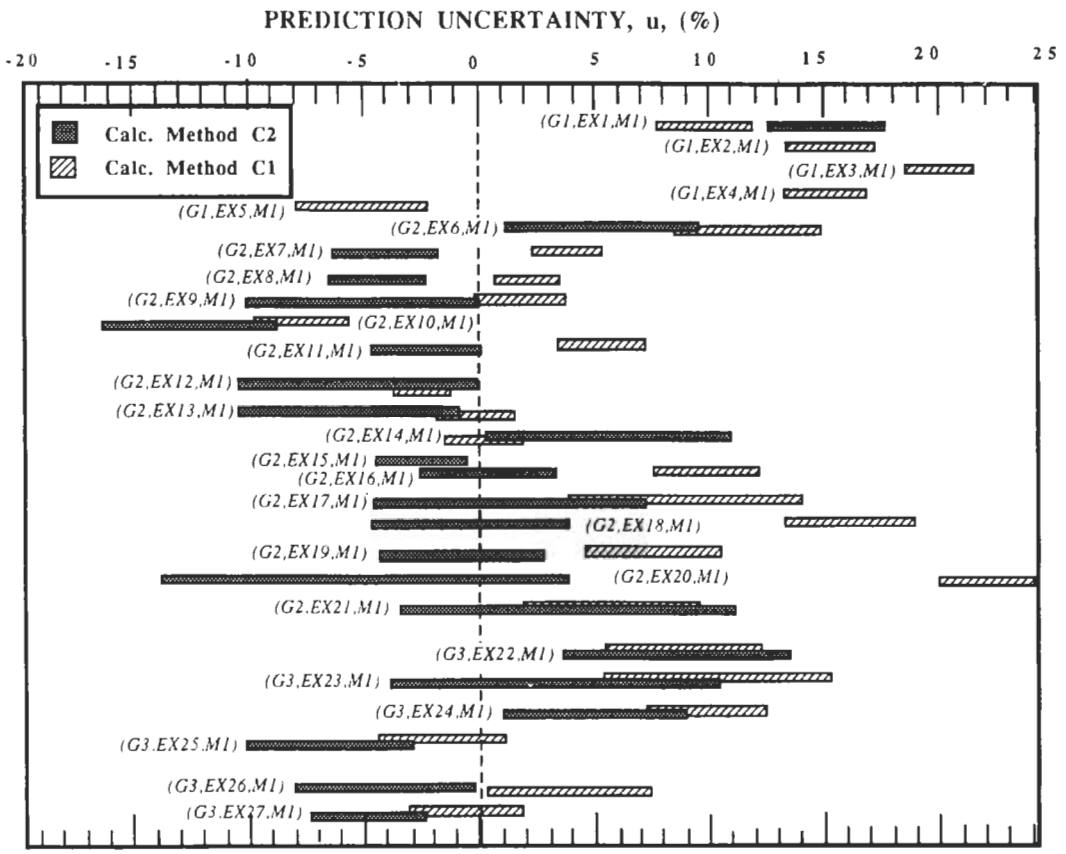

Fig. 3. The prediction uncertainty, u (%), in the response, R, based on measuring method M1.

study the impact of the choice of the interval width on the shape of the NDF, we considered the cases of Δu_j = 2, 2.5, 3.3, and 5%. The NDF in each case is shown in Fig. 7. The corresponding $(CL)_k - S_k$ curves are given in Fig. 8. The confidence level that the calculated response, R, will not exceed measured value in the case of $\Delta u_j = 5\%$ is only ~38% if no safety factor is applied ($S_k = 1$). For other Δu_j, this confidence level is ~42%. To have a confidence level of 100%, S_k should be ~1.3 in the case of $\Delta u_j = 5\%$ and is ~1.28 for $\Delta u_j = 2\%$. (Statistically, no such 100% confidence can be achieved since there are uncertainties in the curves shown in Fig. 7 themselves due to the limited number of cases considered, n, whose magnitude are $\sim 1/n^{1/2}$.) Choosing large interval width tends to give more conservative (larger) safety factors. In all subsequent results, $\Delta u_j = 5\%$ was applied to construct the NDFs.

IV.B. Distinction Between Measuring Methods

The NDFs and the approximating Gaussian curves constructed for other measuring methods are depicted in Figs. 9 and 10. In constructing these curves, results based on both calculational methods C1 and C2 are considered. Note that in doing so, no preference is given to a particular calculational method over the other. The intent in this case, therefore, is to give the overall prediction uncertainty in the response R based on the available calculational techniques applied. Likewise, if no distinction is made between the measuring methods (assuming that all the techniques used to measure the response, R, are reliable in obtaining the measured data), one should consider all the cases shown in Figs. 3 and 4 in constructing the NDF. This overall NDF is shown in Fig. 11. The Gaussian curve that has the same $\bar{u}$ and σ_u of the NDF approximates reasonably well the histogram of the NDF. The overall constructed NDF is mainly driven by the cases for which more measurements are taken by a particular measuring technique, which in our example is the measuring method M1. Table II gives the statistical parameters (the mean uncertainty, $\bar{u}$, the standard deviation, σ_u, the root mean square value, u_{rms}, and the most probable value, u_{mp}) as obtained from the NDFs (not the Gaussians) in each measuring technique case and in the case of combining the results from all measuring methods.

According to Table II, the mean uncertainty, $\bar{u}$, in all cases is positive. This indicates that in our example, it is most likely that the calculations performed to estimate the response R by blanket designers are larger than the actual measured values. When the cases considered in each measuring method are combined, the

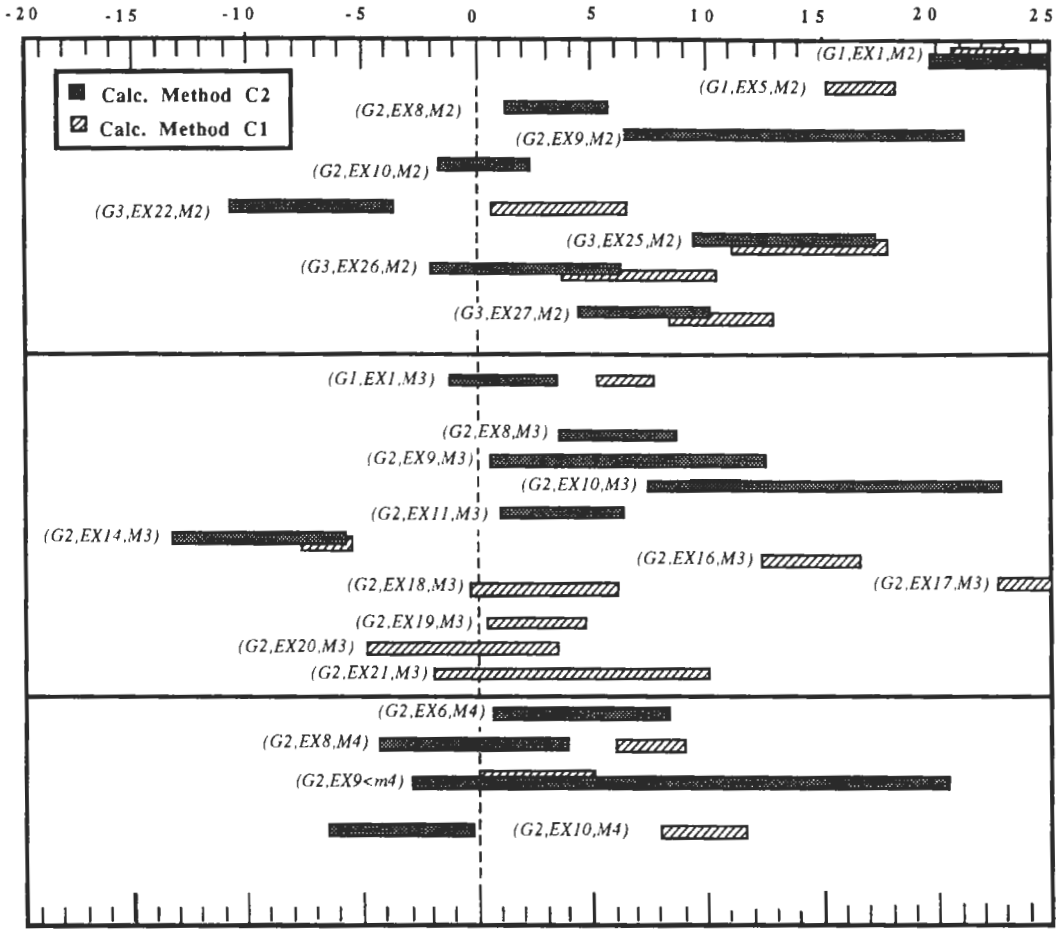

Fig. 4. The prediction uncertainty, u (%), in the response, R, based on measuring method M2, M3, and M4.

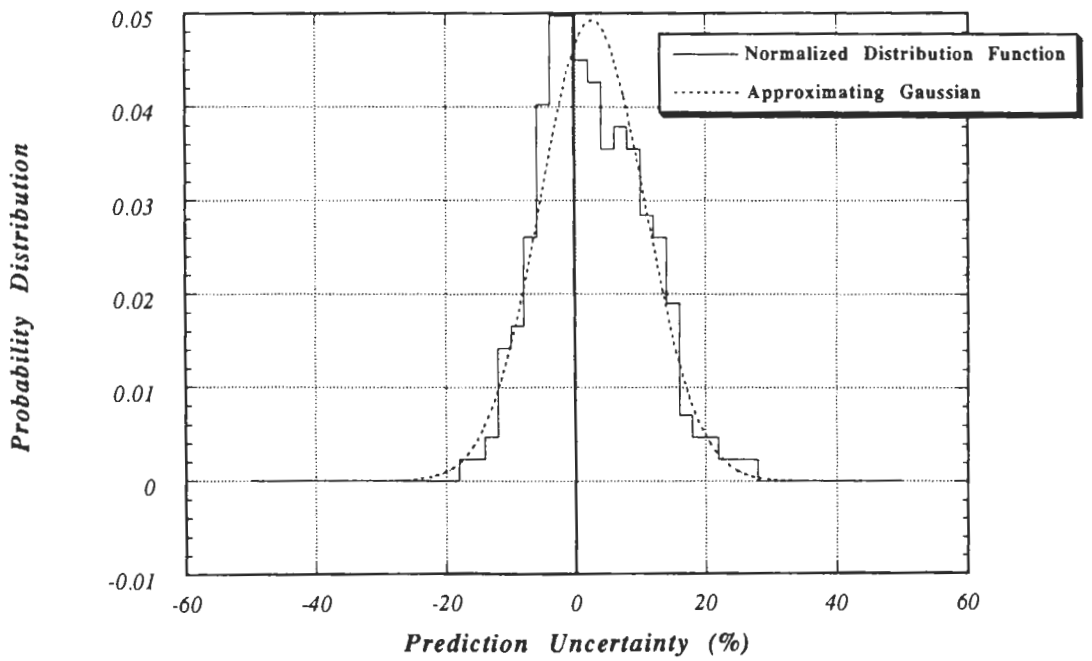

Fig. 5. Normalized density function, f_j, of the prediction uncertainty in the response, R (calculation methods C1 and C2, measuring method M1, all geometries).

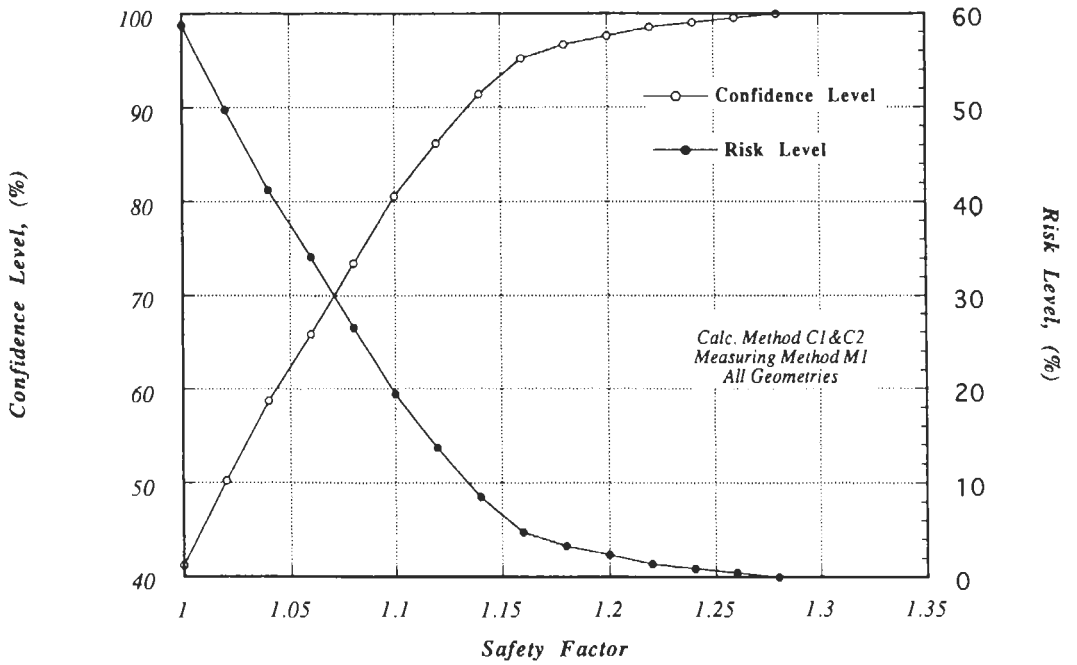

Fig. 6. Confidence and risk levels for the calculations not to exceed measurements as a function of design safety factors for the response, R (calculation methods C1 and C2, measuring method M1, all geometries).

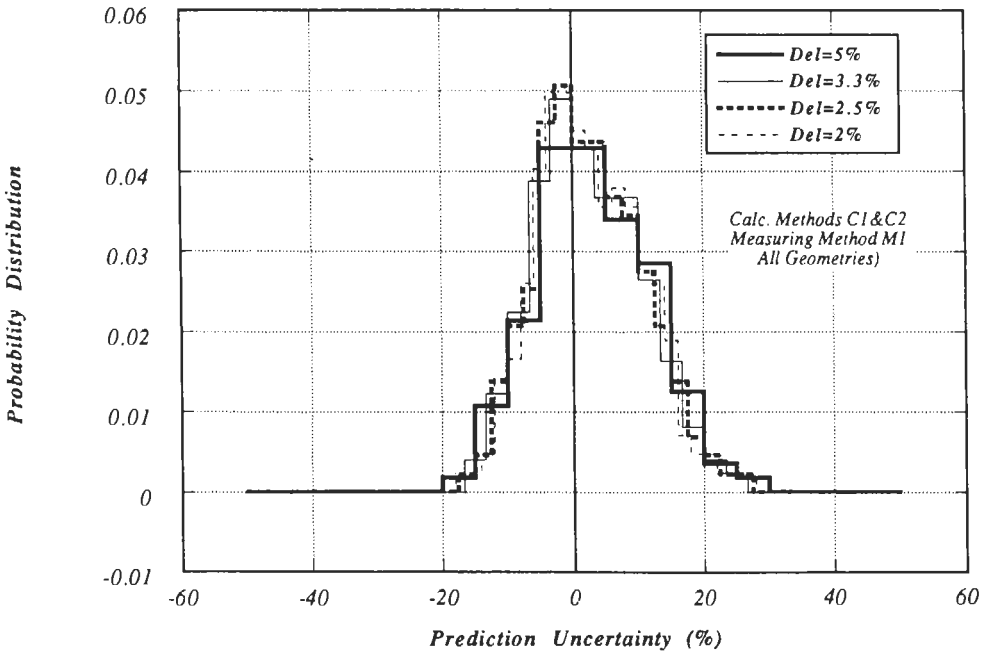

Fig. 7. Effect of interval size on the shape of the normalized density function of the prediction uncertainty in the response, R (calculation methods C1 and C2, measuring method M1, all geometries).

mean prediction uncertainty is ~5% with a standard deviation of ~9%. The derived safety factors are shown in Fig. 12. If no safety factors are used ($S_k = 1$), the confidence levels based on measuring methods M1, M2, M3, M4, and on the results from all measuring methods are ~38%, ~15%, ~23%, ~24%, and ~30%, respectively. All these confidence levels are lower than 50% indicating that the calculation of the response, R, is overpredicted and the least overprediction (larger confidence level) is in the case of the measuring method M1.

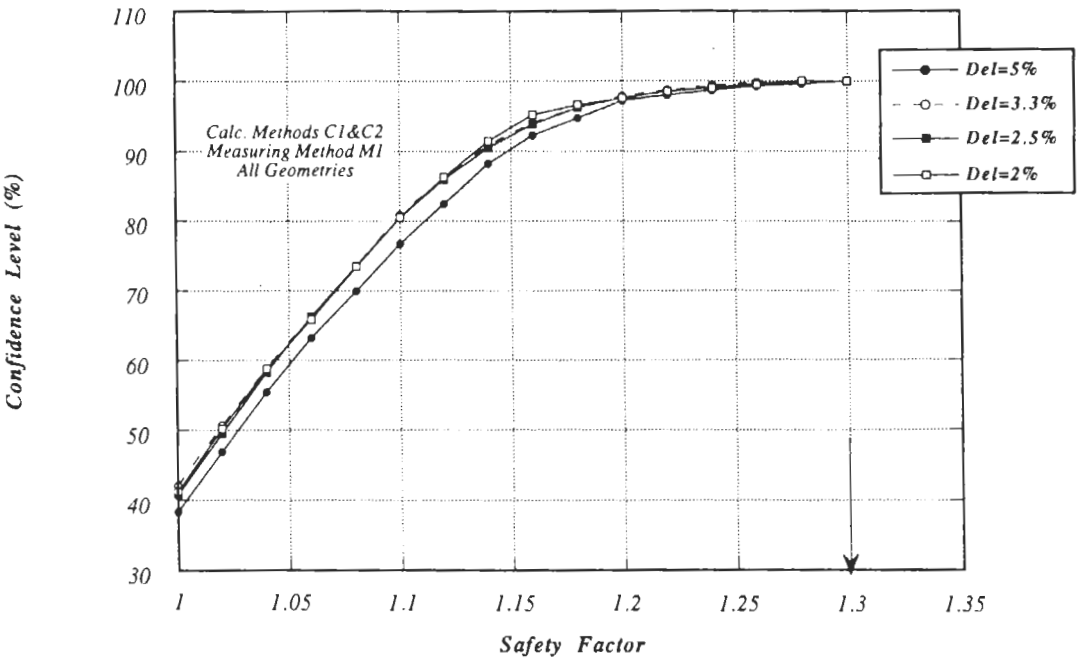

Fig. 8. Effect of interval size on the design safety factors (calculation methods C1 and C2, measuring method M1, all geometries).

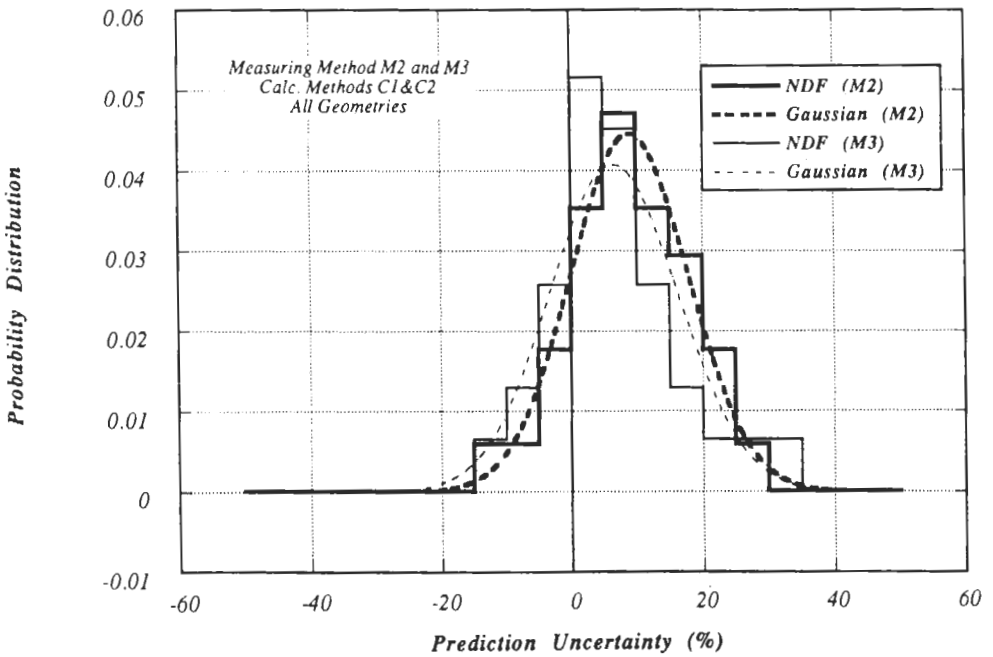

Fig. 9. The NDF of the prediction uncertainty in the response, R (measuring methods M2 and M3, calculation methods C1 and C2, all geometries).

IV.C. Distinction Between Calculational Methods

Distinction can be made between the various calculational methods $\{C1,C2,\ldots,C_{NC}\}$ in deriving the required safety factors. In our example, the required safety factors as a function of the assigned confidence levels are shown in Fig. 13. These factors, based on the calculational methods C1 and C2 treated independently, were evaluated from the NDFs shown in Fig. 14 whose statistical parameters are given in Table III. As

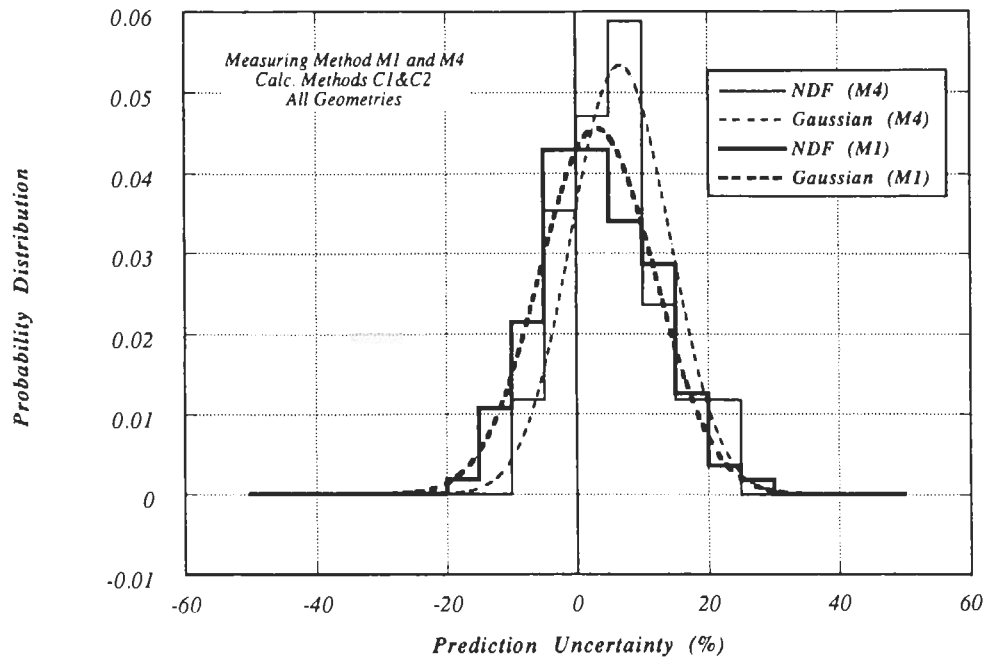

Fig. 10. The NDF of the prediction uncertainty in the response, R (measuring methods M1 and M4, calculation methods C1 and C2, all geometries).

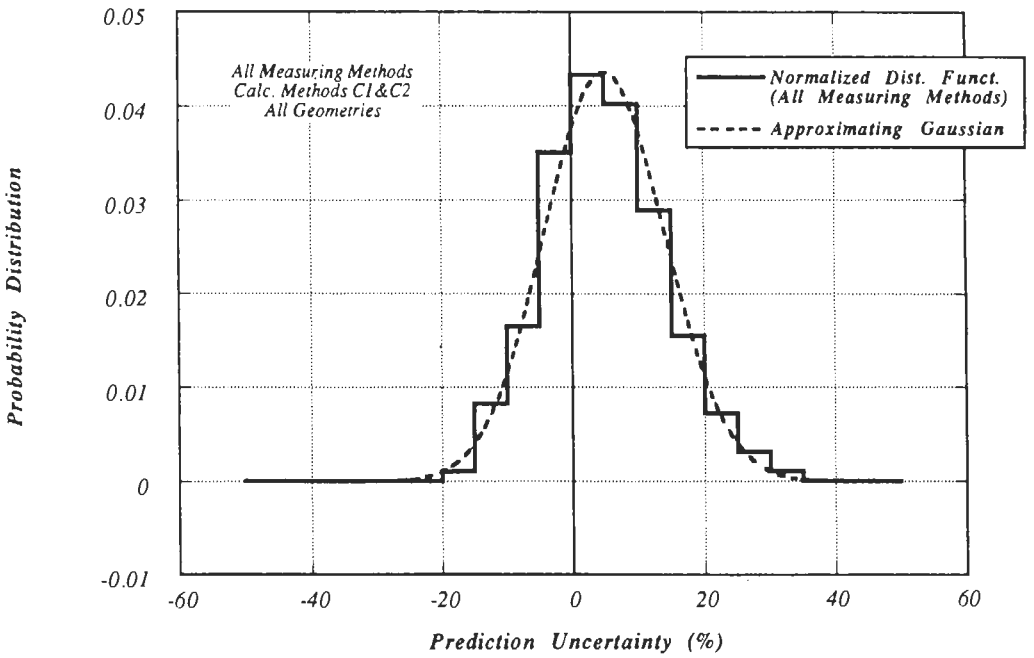

Fig. 11. The NDF of the prediction uncertainty in the response, R (all measuring methods, calculation methods C1 and C2, all geometries).

shown in Table III, $\bar{u}$ based on the C1 and C2 is ~8% and ~2.6%, respectively, (as opposed to ~5% when both methods are considered together) with a spread, σ_u, of ~8% and 9%. This indicates that the C1 method tends to give larger response R by ~5% than that obtained by the C2 method.

IV.D. Distinction Between Various Geometrical Arrangements

One can further make distinction between the various geometrical arrangements $\{G1, G2, \ldots, G_{NG}\}$ in which the response R was measured when deriving the

TABLE II

Statistical Parameters of the Prediction Uncertainty, u (%), of the Response R*

Parameter	Measuring Method				
	Measuring Method M1	Measuring Method M2	Measuring Method M3	Measuring Method M4	All Methods
Number of cases considered	50	15	14	7	86
$\bar{u}$ (average)	3.17	8.97	6.53	5.74	4.95
σ_u (standard deviation)	8.75	8.95	9.79	7.46	9.14
u_{rms} (root mean square)	9.31	12.67	11.77	9.41	10.39
u_{mp} (most probable)	0	7.5	2.5	7.5	2.5

*Calculational methods C1 and C2, all geometries.

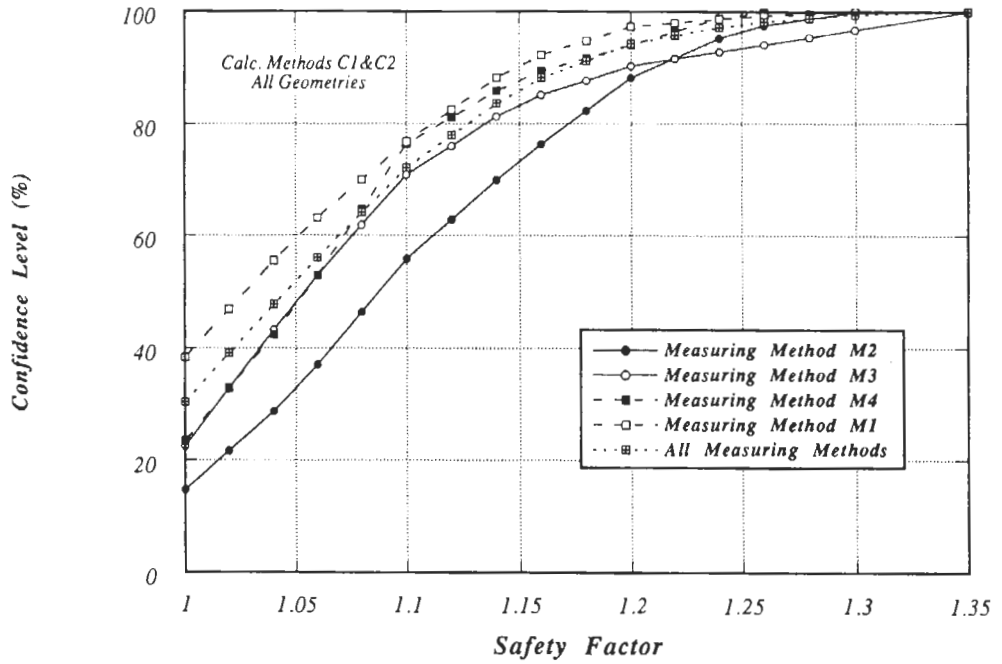

Fig. 12. Confidence level for the calculations not to exceed measurements as a function of design safety factor for the response, R (various measuring methods, calculation methods C1 and C2, all geometries).

TABLE III

Statistical Parameters of the Prediction Uncertainty, u (%), of the Response R as Obtained from Various Calculational Methods (All Measuring Methods, All Geometries)

Method	Discrete Ordinates Method		
	Calc. Method C1	Calc. Method C2	Both Methods
Number of cases considered	43	43	86
$\bar{u}$ (average)	8.03	2.55	4.95
σ_u (standard deviation)	8.08	9.20	9.14
u_{rms} (root mean square)	11.39	9.55	10.39
u_{mp} (most probable)	7.5	−2.5	2.5
Design safety factor (100% confidence)	1.35	1.30	1.35

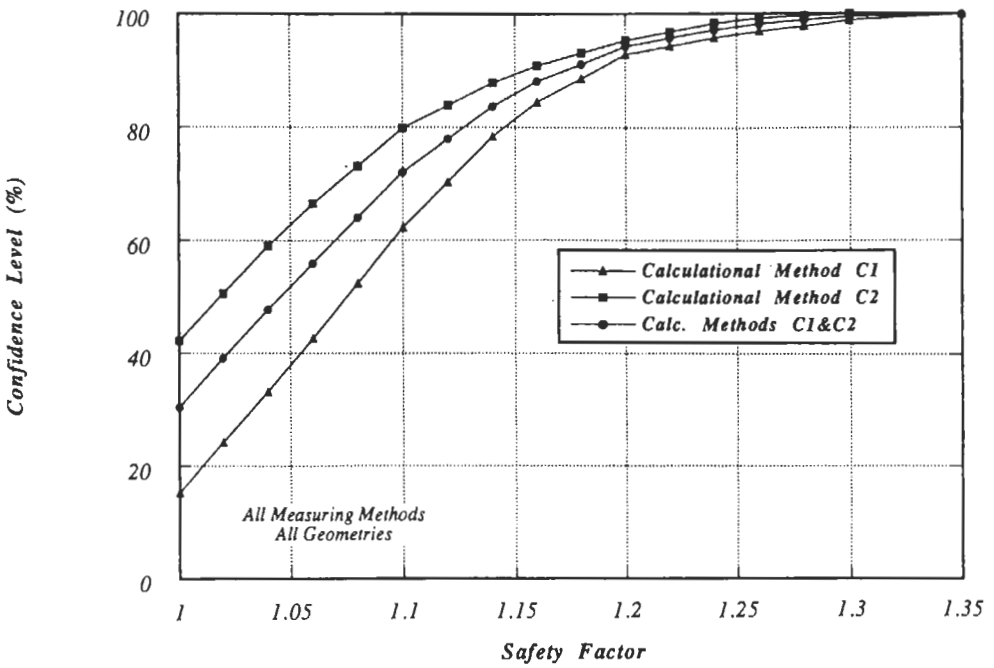

Fig. 13. Effect of the calculational method on the confidence levels and safety factors (all measuring methods, all geometries).

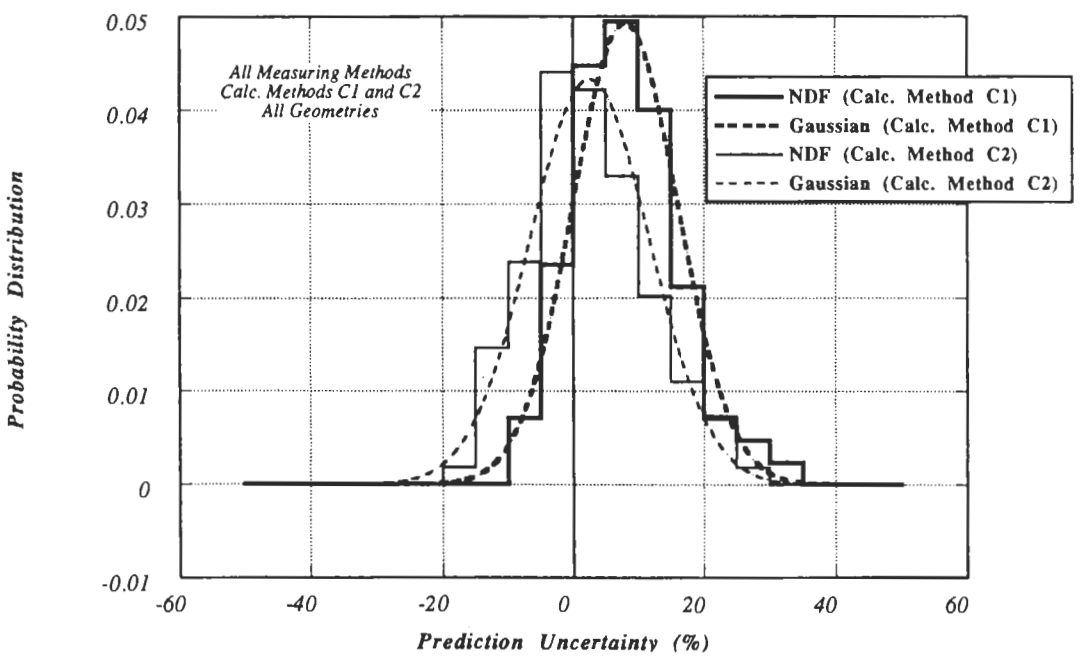

Fig. 14. The NDF of the prediction uncertainty in the response, R, based on calculational methods C1 and C2 (all measuring methods, all geometries).

required safety factors. Table IV gives the statistical parameters pertaining when this distinction is made, and the derived safety factors in this case are shown in Fig. 15. The case when all the geometries are considered together is also given for comparison.

It can be seen from Table IV that the prediction uncertainty $\bar{u}$, is noticeably different in G1 as compared to other geometries. The uncertainty is positive and large in G1 as compared to the corresponding uncertainties in the G2 and G3 cases, which are also positive

TABLE IV

Statistical Parameters of the Prediction Uncertainty, u (%), of the Response R and Dependence on Geometrical Configuration and Dependence on Incident Neutron Spectrum*

Parameter	Geometry			
	G1[a]	G2[a]	G3[a]	All[a]
Number of cases considered	11	55	20	86
$\bar{u}$ (mean)	14.56	3.84	4.50	4.95
σ_u (standard deviation)	8.59	9.04	7.55	9.14
Safety factor (100% confidence)	1.30	1.35	1.20	1.35

*All calculational and measuring methods are considered.
[a]G1: geometry 1, G2: geometry 2, G3: geometry 3, All: all geometries.

but have smaller values of ~4%. It can also be noted from Table IV that the difference between the prediction uncertainty $\bar{u}$ in G2 and G3 is within ~1%. This indicates that by moving from G2 to G3 geometry (there could be a large change in geometry and/or source conditions), the prediction uncertainty of the response, R, has only changed by ~1 to 4% in our example.

V. APPLICATIONS

We give below two applications on the methodology described in Sec. III to derive design safety factors. The first application is on the tritium production rate and the second is a description of an approach to derive these factors from bulk shielding experiments.

V.A. Design Safety Factors for Tritium Production Rates Based on Fusion Integral Experiments

Deriving safety/correction factors for TPR, based on results from integral experiments is the focus subject of the companion paper, Part II (Ref. 59), as obtained from the methodology described here. Numerous experiments on tritium breeding measurements and analysis were performed during the last decade within the U.S. Department of Energy (U.S. DOE)/Japan Atomic Energy Research Institute (JAERI) collaborative program on fusion neutronics[40–49] with the objective of estimating the current uncertainties in TPR prediction. Engineering features found in a fusion blanket (e.g., first wall, coolant channels, beryllium neutron multiplier) have been incorporated in the design of the test assembly so as to quantify the prediction uncertainty in TPR under various design variations. Likewise, the overall geometrical arrangement of the experiments was also varied through Phase I to Phase III of the program. Source conditions of Phases I and II (14-MeV point source) are different from those of Phase III experiments (simulated line source). Details of the experiments and analysis can be referred to in Ref. 59 where the prediction uncertainties in the line-integrated TPR from Li-6 (T6), Li-7 (T7), and natural-Li (Tn) and the design safety factors have been evaluated based on the

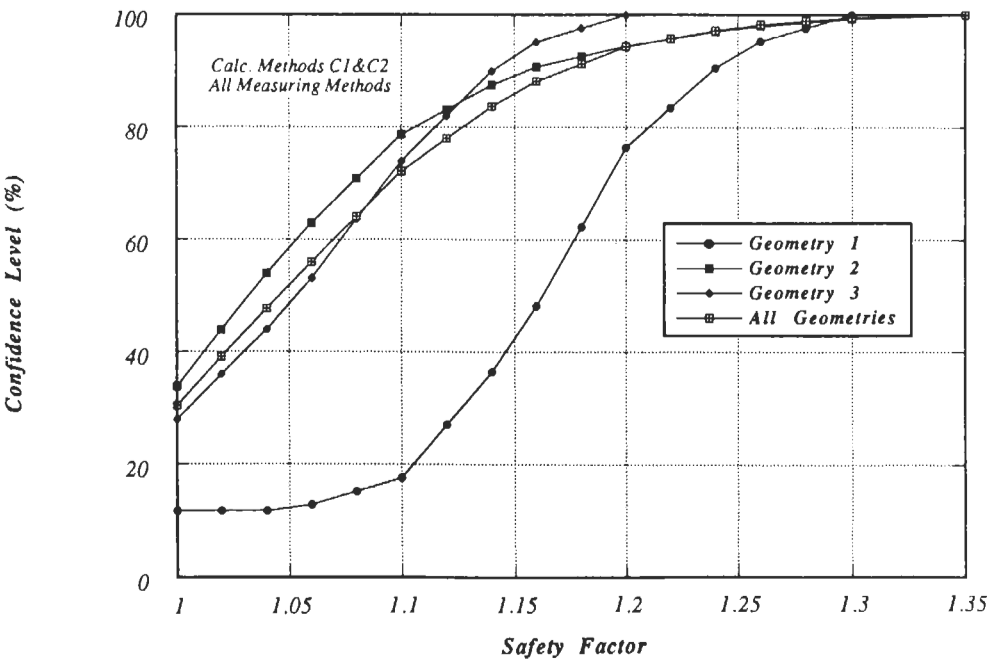

Fig. 15. Effect of geometrical change on the required safety factors for the response, R (calculation methods C1 and C2, all measuring methods).

several databases and codes used independently by the U.S. and JAERI. The line-integrated TPR was chosen as the response since it closely resembles the TBR in a fusion reactor.

The illustrative example given in Sec. IV is indeed for the line-integrated T6 based on the U.S. calculational methods and data. The calculational methods C1 and C2 are the DOT and MCNP results, respectively. The measuring methods M1, M2, M3, and M4 are respectively the Li-glass, Li-pellet, Li-metal, and zonal methods used to measure local T6. Thus all the pertaining results shown in Figs. 3 through 15 and in Tables II through IV are for the prediction uncertainties in the line-integrated T6 where the geometrical arrangements G1, G2, and G3 represent the Phase I, Phase II, and Phase III experimental arrangements, respectively. The prediction uncertainties in the line-integrated T7 and Tn are detailed in Ref. 59.

We note that at present, blanket designers calculate the TBR from Li-6 (C_6) and from Li-7 (C_7) and allow the sum $C_6 + C_7$ to be larger than unity by a margin that covers the uncertainties due to approximations in modeling, calculational methods applied, and present nuclear data uncertainties. As such, blanket designers indirectly use a safety factor in the TBR calculation. The embedded assumption made in this case, which is not realized by blanket designers, is that the calculated TBR could be larger the actual measured value and, therefore, should be reduced by applying the arbitrary safety factor S_k. However, there is a definite risk level associated with each safety factor according to the discussion in Sec. III. For practical purposes, therefore, the following procedures are recommended for TBR calculations in fusion reactors:

1. Construct normalized density functions for TBR from Li-6 and Li-7 based on existing integral measurements and calculations inside test assemblies that closely represent the blanket type under consideration.

2. Choose confidence levels, $(CL)_{k6}$ and $(CL)_{k7}$, for TBR from Li-6 (C_6) and Li-7 (C_7), respectively, ensuring that C_6 and C_7 will not be larger than the actual values, E_6 and E_7.

3. Determine the prediction uncertainties, u_{k6} and u_{k7}, from the normalized density functions, f_{j6}, and f_{j7}, which satisfy the conditions (see Sec. III and Fig. 2)

$$1 - (CL)_{k6} = a_{k6} = \int_{u_{k6}}^{\infty} f_6(u)\,du = \sum_{j6}^{K_6} f_{j6} \qquad (11)$$

$$1 - (CL)_{k7} = a_{k7} = \int_{u_{k7}}^{\infty} f_7(u)\,du = \sum_{j7}^{K_7} f_{j7} \ , \qquad (12)$$

where j_6 and j_7 correspond to the interval in the u_6 and u_7 spaces where u_{k6} and u_{k7} lie, and K_6 and K_7 are the last intervals of the f_{j6} and f_{j7} histograms in the positive u direction.

4. Determine the safety factors S_{k6} and S_{k7} given by $(u_{k6} + 1)$ and $(u_{k7} + 1)$, respectively.

5. Obtain the modified calculated values, C_{mk6} and C_{mk7}, calculated as $C_{mk6} = C_{k6}/S_{k6}$ and $C_{mk7} = C_{k7}/S_{k7}$, respectively.

6. If the sum,

$$TBR = a_6 C_{mk6} + (1 - a_6) C_{mk7}$$

$$(a_6 \equiv \text{Li-6 enrichment}) \ , \qquad (13)$$

falls below a minimum value dictated by satisfying tritium self-sufficiency condition,[1] designers should modify their blanket design by increasing the breeding zone thickness, varying a_6, and/or using a neutron multiplier, and repeating steps 5 to 6 such that the resultant TBR is at least equal to the assigned minimum value.

V.B. An Approach for Determining Design Safety Factors Based on Shielding Experiments and Analysis

There are several technical issues related to shielding design that need to be examined and resolved through integral experiments prior to the construction of a reactor. They are related to the proper protection of sensitive nuclear components as well as protecting personnel against radiation during scheduled and unscheduled maintenance. These issues have been carefully examined[57,58,60] in the process of designing an effective shielding system for ITER (Refs. 61, 62, and 63) during the conceptual design activity (CDA) phase. The adequate protection of the SCM against radiation effects with a limited available space for the inboard shield is an example of such issues. Design responses (parameters) of interest are the following: peak end-of-life fast neutron fluence to SCM, peak end-of-life dose to the organic insulator in the winding pack of the SCM, peak end-of-life copper stabilizer damage due to atomic displacements, peak winding pack power density, and total nuclear heating in coils of the SCM. The concern in this case is that the calculated values could be lower than the actual measured quantities (see Sec. III). Several efforts were made to quantify the uncertainties in these responses that are attributed to the current uncertainties in the nuclear data.[55,56] It was shown, for example, that to cover these uncertainties, an incremental increase in the PCA-shield of ~1.5 to 1.8 cm is required (~2.3 to 2.7 cm in a tungsten-shield type).[55] The economic penalty of this design conservatism is an increase in the total cost of the machine of $10 million to 14 million in the PCA-shield case as opposed to $13 million to 17 million in the case of the W-shield for a machine of ~3-m major radius.[55]

A number of bulk shielding experiments and streaming experiments were conducted to date to verify the prediction capabilities of codes and databases.[64-71] The results from these experiments do not fully cover the perceived difference anticipated between the calculated and

the actual responses in a real reactor, such as ITER. On one hand, this is partly due to the fact that the attenuation characteristics of the shield are a strong function of the exact material selection and the fine details of the design, which, at the moment, are evolving for ITER. On the other, untested safety factors have been routinely used by designers, and they require further verification through dedicated integral experiments. At present, factors used so far by designers to account for inaccuracies in modeling are ~3 for the one-dimensional calculations and ~1.5 for the Monte Carlo calculations. The factors used for gap calculations are 1.6 for local responses and 1.2 for integrated responses.[72] (Note that these factors, F's, are the reciprocal of the safety factors defined in Sec. III, i.e., $F = 1/S_k$.) Below, we describe an approach for determining these safety factors from the results of integral experiments.

V.B.1. Determination of Safety Factors

The methodology outlined in Sec. III could be followed in determining the correction/safety factors from the results of bulk shielding experiments. The response considered, R, could be one of the responses mentioned above which are represented by the responses set $\{R1,R2,\ldots,R_{NR}\}$. Since each of these responses has its own dependence on the neutron and/or gamma flux behind the shield, the derived safety factors will be different. Moreover, the value of each response depends on the depth inside the test assembly where measurements are performed. Figure 16 shows a possible arrangement for bulk shielding experiments. In scenario A, multiple assemblies of different thicknesses $\{X1,X2,\ldots,X_{NX}\}$ are used and the response is measured behind each assembly at the measuring locations $\{P1,P2,\ldots,P_{NP}\}$ in the traverse direction. In scenario B, a single assembly of total thickness, X_{NX}, is used where measurements in the traverse direction are taken at various depths X1, X2, ..., and X_{NX}. In principle, all measurements in scenario B could be performed in the same experiment/assembly while measurements in scenario A are deferred till the required assembly thickness is set up. Note in Fig. 16 that a reflection control component is added to the geometry so as to simulate as closely as possible the actual energy/angular distribution of the incident neutron found in a real reactor, hence, more meaningful safety factors could be derived. It is also important to ensure that the room-returned neutrons from the surroundings are eliminated and do not interfere with the measurements. There may, therefore, be another reflection control component added at the other end of the assembly.

The material arrangement/design details inside the assembly may add another variant to these bulk shielding experiments. For example, safety factors may be derived for the case where the test assembly is made of one material [e.g., stainless steel (SS)] or a combination of two materials (e.g., SS/H_2O at a ratio of 80:20), or three or more materials (SS, H_2O, B_4C, Pb,

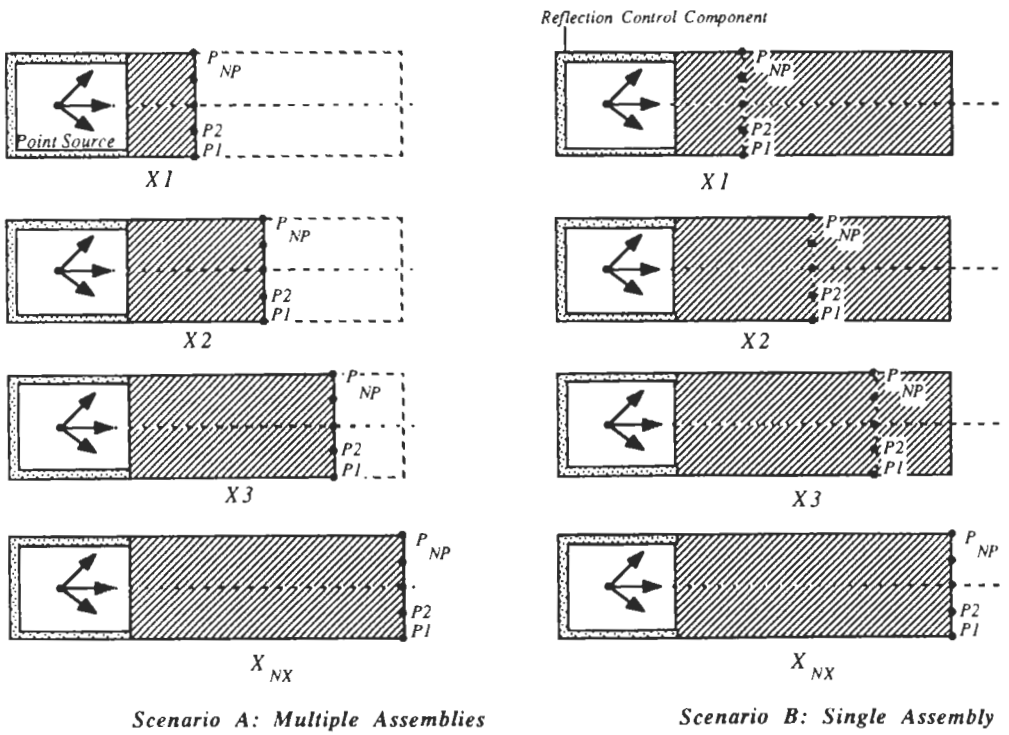

Fig. 16. Possible arrangements and measuring locations in bulk shielding experiments.

Pb/B_4C or W). These geometrical/material arrangements are denoted as the geometry set {G1,G2,..., G_{NG}}. In addition, a particular response, R, could in principle be measured by several measuring methods, which are denoted here as the set {M1,M2,...,M_{NM}}. For example, neutron spectrum measurements could be performed by a small spherical NE213 detector or by a miniature proton recoil counter (PRC) (Ref. 44).

The analysis of the experiments could be performed using different codes and databases. Examples of the currently available transport codes and data sets are given in Sec. II (see also Fig. 1). If the bulk shielding experiments were to be analyzed by several databases, we denote them by the databases set {D1,D2,..., D_{ND}}. Likewise, the calculational method/codes applied are presented by the set {C1,C2,...,C_{NC}}.

Figure 17 shows the proposed procedures to be followed in determining the design safety factors and the associated confidence levels. There are six distinct variants (loops) that represent conditions (cases) under which the NDF is constructed from the prediction uncertainties, u_i, and the associated standard deviations, σ_i, in the response, R, at the measuring points {P1,P2,..., P_{NP}}. For a given response, R, geometry, G, depth inside the assembly, X, measuring method, M, database, D, and calculational method, C, the minimum number of cases from which the NDF is constructed is NP; the number of locations at which the response, R, is measured. However, one can construct the NDF, as desired, from combination of conditions. For example, if it is desired to construct the NDF and safety factors for a particular response, R_p, based on a particular database, D_p, in a particular geometry, G_p, at a particular depth X_p, with no distinction made between any of the calculational methods applied or the measuring methods used, the number of cases from which the NDF is constructed will be NM·NC·NP, where NM and NC are the total number of measuring methods and calculational methods used, respectively. The combination of total calculational methods and measuring methods is given the notation (C) and (M) in Fig. (17). Similar notation is given to the total combination for the other variants, e.g., (R), (D), etc. Partial combinations can also be applied. For example, if it is desired to construct the NDF and safety factors based on the deterministic methods and the Monte Carlo methods, independently, one can use only the pertaining results in each case, which is a sub-set of the total combination case (C). This partial combination is denoted by [CiCj] in Fig. 17. The extreme case is when the NDF and safety factors are determined from all possible cases shown in Fig. 17 combined together. Under this condition, the total number of cases from which the NDF and safety factors are constructed is NR·NG·NX·NM·ND·NC,NP. These factors may not be meaningful but they will give qualitatively overall design margins that do not distinguish between responses, geometry, depth, etc., and are the average of the factors derived for each distinct case, when treated separately.

VI. ON THE VALIDITY OF THE PROPOSED METHODOLOGY

The NDF described in Sec. III is constructed from the mean prediction uncertainty, $u_i = c_i/e_i - 1$ and the spread around it, $\pm\sigma_i$, as found in each experiment, i. The variable considered here is basically c/e. Since neither c nor e is the same in each experiment, which could have a different geometrical arrangement, c or e could not be viewed as a random variable. Furthermore, the choice of different calculational parameters (e.g., number of groups/quadrature in discrete ordinates treatment or the number of histories in Monte Carlo

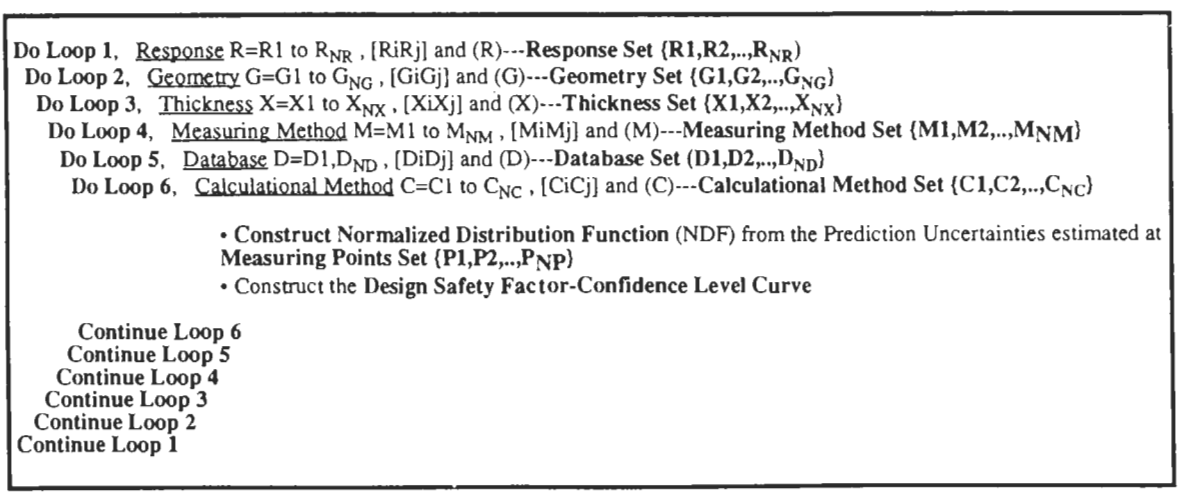

Fig. 17. Procedures for the determination of design safety factors and the associated confidence levels in bulk shielding experiments.

calculations) could lead to a range of possible values for c. Likewise, unidentified systematic errors in measurements are not random. From an abstract statistical viewpoint, the ratio c/e might not be a random variable. Ideally, this ratio should be unity under the conditions of perfect calculational method/modeling, database, and measuring technique. However, both the values of c and e are governed by many factors, examples of which include the value of a particular cross section of a given material in a particular energy range, the choice of the calculational parameters, boundary conditions, and the specific procedures followed in applying a particular measuring technique. Having this many factors, which could be uncontrollable in a large number of situations, could result in de facto randomness of c/e. To be emphasized is that the mean prediction uncertainty, $\bar{u}$, the spread around it, σ_u, and the safety factors defined here are derived from the constructed NDF, which is not necessarily a Gaussian function. We showed in this work that the NDF could in fact approach a Gaussian distribution should the number of experiments (cases) be increased (see also Part II, Ref. 59), indicating the de facto randomness nature of the quantity $c/e - 1$ for the reasons discussed above.

VII. SUMMARY

The role of the neutronics experimentation and analysis in fusion neutronics R&D programs was discussed. This covers obtaining new and/or improving existing nuclear databases, benchmark experiments, and design-oriented integral experiments. The later class lays the bases for quantifying design margins and generating safety factors to be implemented by blanket/shield designers in their design. In this regard, a novel methodology was developed to arrive at estimates to design safety factors based on the experimental and analytical results from existing/proposed integral experiments. In the methodology, and for a particular nuclear response, R, an NDF is constructed from the prediction uncertainties, u_i's, and their associated standard deviations, $\pm\sigma_i$'s, as calculated in various integral experiments where that response is measured. Important statistical parameters are derived from the NDF such as the global mean prediction uncertainty, $\bar{u}$, and the possible spread, $\pm\sigma_u$, around it. The method of how to derive safety factors from many possible NDFs based on various calculational and measuring methods (among other variants) was described. Associated with each safety factor is a confidence level, which designers may choose to have, that the calculated response, R, will not exceed (or will not fall below) the actual measured value. The validity of the proposed approach to obtain these factors was also discussed.

The methodology was applied to two types of nuclear response. In the first, it was shown how to estimate the mean prediction uncertainties and the required safety factors for the line-integrated TPR from Li-6 (T6) as obtained from the U.S. DOE/JAERI collaborative program on fusion neutronics. In the second application, an approach was described on how to derive safety factors from bulk shielding integral experiments. Conditions under which these factors could be derived are the following: type of nuclear response under consideration, type of geometry, shield thickness, measuring methods used, and database and calculational method applied. These factors could also be generated when several conditions are combined.

The process of defining the required neutronics R&D tasks for ITER has already started. It is envisioned that a substantial part of this effort will be devoted to integral experiments on the bulk shield, penetrations, tritium breeding, induced activation, and nuclear heating measurements on design-oriented mock-ups. Determination of the safety factors is the main objective of these experiments. The methodology described in this paper lays the bases for obtaining these factors. It is to be emphasized, however, that for these factors to be meaningful, the size, complexity, and material selection of the mock-ups should have as large a similarity, as possible, to the actual components intended for use in ITER. Furthermore, point sources are the only available nuclear field that produce 14-MeV neutrons since no volumetric 14-MeV source does currently exist, and therefore, extrapolating the results to actual plasma conditions may be needed. This may require further sensitivity studies to connect the results from integral experiments to actual reactor conditions. However, the generated safety factors based on 14-MeV point or simulated line-sources, according to the methodology described in this paper, could be very valuable in qualitatively defining the margins needed for the design.

ACKNOWLEDGMENT

This work was conducted under the U.S. Department of Energy grant DOE-FG03-88ER52150.

REFERENCES

1. M. A. ABDOU, E. L. VOLD, C. Y. GUNG, M. Z. YOUSSEF, and K. SHIN, "DT Fuel Self-Sufficiency in Fusion Reactors," *Fusion Technol.*, **9**, 250 (1986).

2. S. M. QAIM, "Recent Developments in Cross-Section Measurements for Fusion Reactors," *Proc. Int. Conf. Nuclear Data for Science and Technology*, Mito, Japan, May 30–June 3, 1988, p. 179, S. IGARASI, Ed., Japan Atomic Energy Research Institute (1988).

3. A. TAKAHASHI, "Measurements of Double Differential Neutron Emission Cross Sections with 14 MeV Source

for D, Li, Be, C, O, Al, Cr, Fe, Ni, Mo, Cu, Nb, and Pb," *Proc. Conf. Nuclear Data for Science and Technology*, Antwerp, Belgium, September 6–10, 1982, p. 360, D. Reidel Publishing Company, Dordrecht (1983).

4. Y. GOHAR, "Nuclear Data Needs for Fusion Reactors," *Proc. Int. Conf. Nuclear Data for Basic and Applied Science*, Santa Fe, New Mexico, May, 1985, Vol. 1, p. 15, P. G. YOUNG et al., Eds. (1985).

5. E. T. CHENG, "Review of the Nuclear Data Status and Requirements for Fusion Reactors," *Proc Int. Conf. Nuclear Data for Science and Technology*, Mito, Japan, May 30–June 3, 1988, p. 187, S. IGARASI, Ed., Japan Atomic Energy Research Institute (1988).

6. S. GANESAN and D. W. MUIR, "FENDL Multigroup Libraries," IAEA-NDS-129, International Atomic Energy Agency (July 1992).

7. W. A. RHOADES and R. L. CHILDS, "An Updated Version of the DOT 4 (Version 4.3) One-and-Two-Dimensional Neutron/Photon Transport Code," ORNL-5851, Oak Ridge National Laboratory (Apr. 1982); see also CCC-429, Radiation Shielding Information Center (1982).

8. W. A. RHOADES and R. L. CHILDS, "The DORT: Two-Dimensional Discrete Ordinates Transport Code," *Nucl. Sci. Eng.*, **99**, 88 (May 1988); see also CCC-484, Radiation Shielding Information Center (1988).

9. R. E. ALCOUFFE et al., "User's Guide for TWODANT: A Code Package for Two-Dimensional, Diffusion-Accelerated, Neutral-Particle Transport," LA-10049-M, Rev. 1.3, Los Alamos National Laboratory (1986).

10. T. MORI, M. NAKAGAWA, and M. SASAKI, "One-, Two-, and Three-Dimensional Transport Codes Using Multi-Group Double-Differential Form Cross Sections," JAERI-1314, Japan Atomic Energy Research Institute (Nov. 1988).

11. G. PALMIOTTI and M. SALVATORES, "Optimized Two Dimensional Sn Transport (BISTRO)," presented at Int. Topl. Mtg. Reactor Physics, Paris, France, April 27–30, 1987.

12. LOS ALAMOS MONTE CARLO GROUP, "MCNP—A General Monte Carlo Code for Neutron and Photon Transport," Version 3A, LA-7396, Rev. 2, Los Alamos National Laboratory (1986).

13. M. NAKAGAWA and T. MORI, "MORSE-DD, A Monte Carol Code Using Multigroup Double Differential Form Cross-Sections," JAERI-M84-126, Japan Atomic Energy Research Institute (July 1984).

14. T. MORI, M. NAKAGAWA, and M. SASAKI, "Vectorization of Continuous Energy Monte Carlo Method for Neutron Transport Calculation," *J. Nucl. Sci. Technol.*, **29**, *4*, 325 (Apr. 1992).

15. J. C. NIMAL et al., "TRIPOLI-2, Programme de Monte Carlo Polycinétique à trois dimensions, Tomes I,II, III," DEMT/86/239, SERMA/LEPF/86/789, DEMT/86/240, SERMA/LEPF/86/799, Commissariat à l'Energie Atomique.

16. J. JUNG, "Theory and Use of the Radioactivity Code RACC," ANL/FPP/TM-122, Argonne National Laboratory (May 1979).

17. D. HENDERSON and O. YASAR, "DKR-ICF: A Radioactivity and Dose Rate Calculation Code Package," UWFDM-714, Vols. 1 and 2, University of Wisconsin (Nov. 1987).

18. Y. FARAWILA, Y. GOHAR, and C. MAYNARD, "KAOS-V Code: An Evaluation Tool for Neutron Karma Factors and Other Nuclear Responses," ANL/FPP/TM-240, and "KAOS/LIB-V: A Library of Nuclear Response Functions Generated by KAOS-V Code from ENDF/B-V and Other Data Files," ANL/FPP/TM-241, Argonne National Laboratory (1989).

19. Y. SEKI, H. IIDA, H. KAWASAKI, and K. YAMADA, "THIDA-2: An Advanced Code System for Calculation of Transmutation, Activation, Decay Heat and Dose Rate," JAERI 1301, Japan Atomic Energy Research Institute (Mar. 1986).

20. C. R. WEISBIN et al., "Application of FORSS Sensitivity and Methodology to Fast Reactor Benchmark Analysis, ORNL/TM-5563, Oak Ridge National Laboratory (1976); see also "FORSS: A Sensitivity and Uncertainty Analysis Code System," CCC-334, Radiation Shielding Information Center, Oak Ridge National Laboratory (1983).

21. M. EMBRECHTS, "SENSIT-2D: A Two-Dimensional Cross-Section Sensitivity and Uncertainty Analysis Code," LA-9515-MS, UC-32, Los Alamos National Laboratory (Oct. 1982).

22. A. KUMAR, M. A. ABDOU, and J.-P. SCHNEEBERGER, "Integral Fusion Neutronics Experiments and Analysis," *Proc. Topl. Mtg. New Horizons in Radiation Protection and Shielding*, Pasco, Washington, April 26–May 1, 1992, p. 619, American Nuclear Society (1992).

23. T. NAKAMURA and K. SUGIYAMA, "Integral Experiments for Fusion Reactors," *Proc. Int. Conf. Nuclear Data for Science and Technology*, Mito, Japan, May 30–June 3, 1988, p. 171, S. IGARASI, Ed., Japan Atomic Energy Research Institute (1988).

24. Y. OYAMA and H. MAEKAWA, "Measurements and Analysis of an Angular Neutron Flux on a Beryllium Slab Irradiated with Deuterium-Tritium Neutrons," *Nucl. Sci. Eng.*, **97**, 220 (1987).

25. H. MAEKAWA and Y. OYAMA, "Experiment on Angular Flux Spectra from Lead Slabs Bombarded by D-T Neutrons," *Fusion Eng. Des.*, **18**, 287 (1991).

26. V. A. ZAGRYADSKIJ et al., "Measurements of Neutron Leakage from U, Th, and Be Spherical Assemblies with a Central 14 MeV Source," INDC(CCP)-272/G, International Atomic Energy Agency (1987).

27. C. ICHIHARA et al."Measurements of Leakage Neutron Spectra from Various Spherical Piles of Five Elements with 14 MeV Neutrons," *Proc. 2nd Int. Workshop Fusion Neutronics*, June 5, 1992, UCLA-FNT-60, ENG-93-15, University of California at Los Angeles (1992); see also C. ICHIHARA et al., *Proc Int. Conf. Nuclear Data for Science and Technology*, Mito, Japan, May 30-June 3, 1988, S. IGARASHI, Ed., Japan Atomic Energy Research Institute (1988).

28. K. SUMITA et al., "Integral Benchmark Experiments on Be-Li Graphite Systems for Tritium Breeding Blanket Design," *Fusion Eng. Des.*, **18**, 355 (1991).

29. J. W. DAVIDSON and M. E. BATTAT, "Calculation of the INEL Beryllium Multiplication Experiment," *Fusion Technol.*, **19**, Suppl. B, 2007 (1991).

30. Y. CHEN et al., "Experiments of Neutron Multiplication in Beryllium," *Fusion Technol.*, **19**, Suppl. B, 1919 (1991).

31. U. FISCHER, A. SCHWENK-FERRERO, and E. WIEGNER, "Analyses of the 14 MeV Neutron Transport in Beryllium," *Fusion Eng. Des.*, **18**, 361 (1991).

32. S. YAMAGUCHI, H. MAEKAWA, K. KOSAKO, and T. NAKAMURA, "Measurements of Gamma-Ray Heating in Lithium-Oxide, Graphite, and Iron Slab Assemblies Bombarded by D-T Neutrons," *Fusion Eng. Des.*, **10**, 163 (1989).

33. A. KUMAR, M. Z. YOUSSEF, M. A. ABDOU, Y. IKEDA, C. KONNO, Y. OYAMA, and T. NAKAMURA, "Direct Nuclear Heating Measurements in Fusion Neutron Environment and Analysis," *Fusion Eng. Des.*, **18**, 397 (1991).

34. Y. IKEDA et al., "Measurement and Analysis of Nuclear Heat Depositions in Structural Materials Induced by D-T Neutrons," *Fusion Technol.*, Suppl. A-B, **21**, 2190 (1992).

35. M. A. ABDOU and C. W. MAYNARD, "Calculation Methods for Nuclear Heating—Part I: Theoretical and Computational Algorithms," *Nucl. Sci. Eng.*, **56**, 360 (1975).

36. A. KUMAR, M. YOUSSEF, Y. IKEDA, C. KONNO, and Y. OYAMA, "Experiments and Analysis for Measurements of Decay Heat Related Induced Activities in Simulated Line Source Driven D-T Neutron Fields of Phase IIIA: JAERI/USDOE Collaborative Program on Fusion Neutronics Experiments," *Fusion Technol.*, **19**, 1859 (1991).

37. Y. IKEDA, C. KONNO, Y. OYAMA, T. NAKAMURA, A. KUMAR, M. Z. YOUSSEF, and M. A. ABDOU, "Experimental Verification of Current Data and Methods for Induced Radioactivity and Decay Heat Calculation in D-T Fusion Reactors," *Fusion Eng. Des.*, **18**, 387 (1991).

38. Y. IKEDA and M. Z. YOUSSEF, "Two-Dimensional Cross-Section Sensitivity and Uncertainty Analysis for Tritium Production Rate in Fusion-Oriented Integral Experiments," *Fusion Technol.*, **13**, 616 (1988).

39. P. M. SONG, M. Z. YOUSSEF, and M. ABDOU, "A New Approach and Computational Algorithm for Sensitivity/Uncertainty Analysis for SED and SAD with Application to Integral Experiments," *Nucl. Sci. Eng.*, **113**, 339 (1993).

40. H. MAEKAWA and M. A. ABDOU, "Overview of Latest Experiments Under the JAERI/USDOE Collaborative Program on Fusion Neutronics," *Fusion Eng. Des.*, **18**, 275 (1991).

41. M. Z. YOUSSEF, C. GUNG, M. NAKAGAWA, T. MORI, K. KOSAKO, and T. NAKAMURA, "Analysis and Intercomparison for Phase I Fusion Integral Experiments at the FNS Facility," *Fusion Technol.*, **10**, 549 (1986).

42. Y. OYAMA, K. TSUDA, S. YAMAGUCHI, Y. IKEDA, C. KONNO, H. MAEKAWA, and T. NAKAMURA, "Phase II Experimental Results of JAERI/USDOE Collaborative Program on Fusion Blanket Neutronics Experiments," *Fusion Eng. Des.*, **9**, 309 (1989).

43. M. Z. YOUSSEF, Y. WATANABE, M. A. ABDOU, M. NAKAGAWA, T. MORI, K. KOSAKO, and T. NAKAMURA, "Comparative Analysis for Phase IIA and IIB Experiments of the U.S./JAERI Collaborative Program on Fusion Blanket Neutronics," *Fusion Technol.*, **15**, 1299 (1989).

44. Y. OYAMA et al., "Phase-IIC Experiments of the USDOE/JAERI Collaborative Program on Fusion Blanket Neutronics—Experiments and Analysis of the Heterogeneous Fusion Blankets—Volume I: Experimental Results," JAERI-M-92-182, Japan Atomic Energy Research Institute (Dec. 1992); see also UCLA-FNT-63, UCLA-ENG-93-18, University of California at Los Angeles (Dec. 1992).

45. M. Z. YOUSSEF et al., "Phase-IIC Experiments of the USDOE/JAERI Collaborative Program on Fusion Blanket Neutronics—Experiments and Analysis of the Heterogeneous Fusion Blankets—Volume II: Analysis," UCLA-FNT-64, UCLA-ENG-93-19, University of California at Los Angeles (Dec. 1992); see also M. NAKAGAWA et al., JAERI-M-92-183, Japan Atomic Energy Research Institute (Dec. 1992).

46. M. Z. YOUSSEF, Y. WATANABE, A. KUMAR, Y. OYAMA, and K. KOSAKO, "Analysis for the Simulation of a Line Source by a 14 MeV Moving Point Source and Impact on Blanket Characteristics: The USDOE/JAERI Collaborative Program on Fusion Neutronics," *Fusion Technol.*, **19**, Suppl. B, 1843 (1991).

47. Y. OYAMA et al., "Phase III Experimental Results of JAERI/USDOE Collaborative Program on Fusion Neutronics," *Fusion Eng. Des.*, **18**, 203 (1991).

48. M. Z. YOUSSEF, A. KUMAR, M. A. ABDOU, Y. OYAMA, K. KOSAKO, and T. NAKAMURA, "Post-Analysis for the Line Source Phase IIIA Experiments of the

USDOE/JAERI Collaborative Program on Fusion Neutronics," *Fusion Eng. Des.*, **18**, 265 (1991).

49. M. Z. YOUSSEF et al., "The Nuclear Analysis of an Annular Li_2O Blanket System Surrounding an Artificially Simulated 14-MeV Line Source and Comparison of Calculation to Measurements," *Fusion Technol.*, **28**, 320 (1995).

50. A. KUMAR, W. R. LEO, L. GREEN, and G. L. WOODRUFF, "Measurements and Analysis of Transmitted Spectra from LOTUS Fission-Suppressed Hybrid Blanket Driven by D-T Neutrons," *J. Fusion Energy*, **8**, 107 (1989).

51. S. AZAM, M. SCHAER, J.-P. SCHNEEBERGER, and A. KUMAR, "Neutronics Studies of Fusion Blankets: Results on a Simulated Lithium-Lead Module," *Fusion Technol.*, **20**, 888 (1991).

52. T. ELFRUTH, J. HANKE, K. SEIDEL, and S. UNHOLZER, "First Intermediate Report: Specification and Optimization of Experimental Set-up and Procedure," *Proc. Informal Int. Mtg. Fusion Neutronics*, June 4-5, 1992, UCLA-FNT-60, ENG-93-15, p. 298, University of California at Los Angeles (Aug. 1992).

53. K. SUMITA, A. TAKAHASHI, T. IIDA, and J. YAMAMOTO, "Status of OKTAVIAN I and Proposal for OKTAVIAN II," *Nucl. Sci. Eng.*, **106**, 249 (1990).

54. G. SHATALOV, "Shielding Experiments with 14 MeV Neutron Source in USSR," *Proc. Int. Workshop Fusion Neutronics*, Karlsruhe, Germany, June 7, 1991, Memo 03-305, p. 35, Japan Atomic Energy Research Institute (Sep. 1991).

55. M. Z. YOUSSEF and Y. OYAMA, "Required Design Margins and Their Economic Impact in Fusion Reactors to Compensate for Nuclear Data Uncertainties – A Global Approach to Define Safety Factors Based on Integral Experiments," *Proc. Int. Conf. Nuclear Data for Science and Technology*, Gatlinburg, Tennessee, May 7-13, 1994 (1994).

56. M. Z. YOUSSEF and I. JUN, "Comparison of PCA Versus Tungsten in TIBER-II In-Board Shield and Impact of Nuclear Data Uncertainties on Machine Cost," *Fusion Technol.*, **15**, 887 (1989).

57. L. A. EL-GUEBALY, "Magnet Shielding Effectiveness of the Proposed Blankets for ITER," *Proc. 14th IEEE/NPSS Symp. Fusion Engineering*, San Diego, California, Sep. 30-Oct. 3, 1991 (1991).

58. L. A. EL-GUEBALY and M. E. SAWAN, "Shielding Considerations for ITER: Current Status and Future Directions," *Proc. Conf. New Horizon in Radiation Protection and Shielding*, Pasco, Washington, April 26-May 1, 1992 (1992).

59. M. Z. YOUSSEF et al., "Fusion Integral Experiments and Analysis and the Determination of Design Safety Factors – II: Application to the Prediction Uncertainty of Tritium Production Rate from the U.S. DOE/JAERI Collaborative Program on Fusion Blanket Neutronics," *Fusion Technol.*, **28**, 388 (1995).

60. W. DAENNER et al., "Neutron Shielding and Its Impact on the ITER Machine Design," *Fusion Eng. Des.*, **16**, 183 (1991).

61. "ITER Conceptual Design Report," ITER Documentation Series, No. 18, International Atomic Energy Agency (1991).

62. A. J. GLASS, "Status and Plans for ITER," *J. Fusion Energy*, **11**, *2* (1992).

63. G. E. SHATALOV et al., "Breeder and Test Blankets in ITER," *Fusion Eng. Des.*, **16**, 85 (1991).

64. K. OISHI, Y. IKEDA, and T. NAKAMURA, "Measurement and Analysis of Neutron Spectra in a Large Cylindrical Iron Assembly Irradiated by 14 MeV Neutrons," *Proc. 7th Int. Conf. Radiation Shielding*, Bournmouth, England, September 12-16, 1988 (1989).

65. Y. IKEDA, K. OISHI, C. KONNO, and T. NAKAMURA, "Neutronics Experiments and Analysis on a Tungsten Slab Assembly Bombarded with D-T Neutrons," *Fusion Eng. Des.*, **18**, 309 (1991).

66. C. KONNO et al., "Measurements and Analysis of Low Energy Neutron Spectrum in a Large Cylindrical Iron Assembly Bombarded by D-T Neutrons," *Fusion Eng. Des.*, **18**, 297 (1991).

67. Y. SEKI et al., "Monte Carlo Analysis of a Streaming Experiment of D-T Neutron and Gamma Rays Through a Concrete Bent Duct," *Proc. 6th Int. Conf. Radiation Shielding*, Tokyo, Japan, May 16-20, 1983.

68. H. NAKASHIMA, S. TANAKA, and H. MAEKAWA, "Experiments and Calculations of 14 MeV Neutron Streaming Through Multi-Layered Slit Assembly," *J. Nucl. Sci. Technol.*, **24**, *8* (Aug. 1987).

69. Y. OKA, K. SHIN, J. YAMAMOTO, and A. TAKAHASHI, "Fusion Neutron Streaming Benchmark Experiment at OKTAVIAN," *Proc. Topl. Mtg. New Horizons in Radiation Protection and Shielding*, Pasco, Washington, April 26-May 1, 1992, p. 643, American Nuclear Society (1992).

70. H. MAEKAWA and C. KONNO, "JAERI R&D Plan for ITER/EDA (Shielding Experiment)," *Proc. Int. Workshop Fusion Neutronics*, Karlsruhe, Germany, June 7, 1991, memo 03-305, Japan Atomic Energy Research Institute (Sep. 1991).

71. C. KONNO, "Status of Shielding Experiment for ITER-Experiments," *Proc. Informal Int. Mtg. Fusion Neutronics*, June 4-5, 1992, UCLA-FNT-60, ENG-93-15, p. 184, University of California at Los Angeles (Aug. 1992).

72. W. DAENNER et al., *Proc. ITER Expert Mtg. Shielding Experiments and Analysis*, Garching, Germany, February 12-14, 1990, ITER-IL-BL-5-0-5 (Mar. 1990).

Mahmoud Z. Youssef (PhD, nuclear engineering, University of Wisconsin, 1980) is a senior research engineer in the Department of Mechanical, Aerospace, and Nuclear Engineering at the University of California, Los Angeles (UCLA). He participated in several conceptual magnetic fusion energy and inertial fusion energy reactor design studies with emphasis on nuclear analysis and blanket/shield design. His research interests are in the areas of blanket/shield design optimization, nuclear data, sensitivity/uncertainty studies, neutronics methods and code development, tritium fuel cycle, radioactivity and safety aspects of fusion, integral experiments, neutronics testing, and research and development for fusion reactors, particularly the International Thermonuclear Experimental Reactor (ITER).

Anil Kumar (PhD, University of Bombay, India, 1981) is senior development engineer at UCLA. His current research interests include fusion reactor nucleonics experiments and analysis, technique development for nuclear heating, decay heat measurements, biological dose, fusion diagnostics, safety factor methodology for fusion reactor design parameters, low-activation materials, inertial confinement fusion, and sequential reactions. He has conducted experiments at leading facilities such as the Fusion Neutronics Source (FNS) facility in Japan, the Tokamak Fusion Test Reactor (TFTR) at Princeton University, and LOTUS in Switzerland.

Mohamed A. Abdou is a professor in the Department of Mechanical, Aerospace, and Nuclear Engineering at UCLA and also is the director of fusion technology at UCLA. His research interests include neutronics, thermomechanics, fusion technology, and reactor design and analysis. He served as the U.S. leader of the Japan Atomic Energy Research Institute (JAERI)/U.S. Department of Energy (U.S. DOE) collaboration on fusion blanket neutronics.

Yukio Oyama (BS, physics, 1975; MS, nuclear physics, 1977; and Dr. Eng., 1989, Osaka University, Japan) is a principal scientist at JAERI. He has worked in the area of fusion neutronics experiments since 1978. He is currently involved in intense and high-energy neutron source projects.

Hiroshi Maekawa (BE, 1965; MS, 1967; and Dr. Eng., 1970, nuclear engineering, Tokyo Institute of Technology, Japan) is the deputy director of the Department of Reactor Engineering and the head of the Intense Neutron Source Laboratory at JAERI. He has worked on fusion neutronics for more than 20 years, and he planned and constructed the FNS facility. He served as the Japanese leader of the JAERI/U.S. DOE collaboration on fusion blanket neutronics. His recent research has focused on International Fusion Materials Irradiation Facility conceptual design activities.